

- human hematopoietic stem and progenitor cells with AMD3100, a CXCR4 antagonist. *J Exp Med* 2005, 201:1307-1318
37. Capoccia BJ, Shepherd RM, Link DC: G-CSF and AMD3100 mobilize monocytes into the blood that stimulate angiogenesis in vivo through a paracrine mechanism. *Blood* 2006, 108:2438-2445
38. Yamaguchi J, Kusano KF, Masuo O, Kawamoto A, Silver M, Mura-sawa S, Bosch-Marce M, Masuda H, Losordo DW, Isner JM, Asahara T: Stromal cell-derived factor-1 effects on ex vivo expanded endo-thelial progenitor cell recruitment for ischemic neovascularization. *Circulation* 2003, 107:1322-1328
39. Misao Y, Takemura G, Arai M, Ohno T, Onogi H, Takahashi T, Minatoguchi S, Fujiwara T, Fujiwara H: Importance of recruitment of bone marrow-derived CXCR4⁺ cells in post-infarct cardiac re-pair mediated by G-CSF. *Cardiovasc Res* 2006, 71:455-465



Effective uptake of *N*-acetylglucosamine-conjugated liposomes by cardiomyocytes *in vitro*

Shin-ichi Aso^a, Hirohiko Ise^{a,*}, Masafumi Takahashi^a, Satoshi Kobayashi^a, Hajime Morimoto^a,
Atsushi Izawa^a, Mitsuaki Goto^b, Uichi Ikeda^a

^a Division of Cardiovascular Sciences, Department of Organ Regeneration, Shinshu University Graduate School of Medicine, 3-1-1 Asahi, Matsumoto, Nagano 390-8621, Japan

^b Celagix Research Ltd., 5800-3 Nagatsuta-cho, Midori-ku, Yokohama, Kanagawa, 226-0026, Japan

Received 12 February 2007; accepted 5 July 2007

Available online 12 July 2007

Abstract

A drug delivery system (DDS) that targets the injured myocardium would serve as a novel therapeutic tool for cardiac diseases. To develop such a DDS, we investigated the interaction of 2 types of glycoside-conjugated liposomes containing a fluorescence substrate with cardiomyocytes. Flow cytometry revealed that cardiomyocytes adequately interact with *N*-acetylglucosamine-conjugated liposomes (GlcNAc-Ls). Furthermore, to confirm whether the agents encapsulated in GlcNAc-Ls affect the intracellular environment of cardiomyocytes, we prepared GlcNAc-Ls-containing pravastatin and examined the effect of pravastatin on cardiomyocytes. Pravastatin is a 3-hydroxy-3-methylglutaryl-CoA reductase inhibitor (statin) and is hydrophilic. It is reported that lipophilic statins enhance nitric oxide (NO) production and inducible nitric oxide synthase (iNOS) expression by interleukin-1 β (IL-1 β)-stimulated cardiomyocytes. The hydrophilic nature of pravastatin prevents its entry into cardiomyocytes; therefore, it cannot enhance both these processes. Treatment with GlcNAc-Ls-containing pravastatin specifically enhanced NO production and iNOS expression by IL-1 β -stimulated cardiomyocytes. Based on these results, we found that cardiomyocytes exhibit a high degree of interaction with GlcNAc-Ls, and GlcNAc-Ls-encapsulated agents can be effectively taken up by cardiomyocytes. We suggest that GlcNAc-Ls can be utilized therapeutically as a DDS for the injured myocardium.

© 2007 Elsevier B.V. All rights reserved.

Keywords: Lectin; Cardiomyocytes; *N*-acetylglucosamine; Liposomes; Drug delivery

1. Introduction

A drug delivery system (DDS) that targets the injured myocardium has great potential to serve as a novel therapeutic tool for myocardial infarction; however, an efficient myocardium-targeted DDS has not been established to date. Different ligands that target cell-surface receptors have been used to improve the specificity of DDSs [1–5]. To develop a DDS that targets the injured myocardium, we focused on a cell-surface lectin expressed by cardiomyocytes and hypothesized that the interaction between lectin and glycoside-conjugated agents could be utilized as a base for the development of this DDS.

Lectins are known to bind glycoside residues, and the cell-surface lectins that bind ligands are internalized into cells and then delivered to intracellular acidic compartments [4,6]. Therefore, targeting cell-surface lectins is a potential strategy for improving both the specificity and efficacy of DDSs [1,4,5,7,8]. However, cell-surface lectins that are expressed by cardiomyocytes and by glycosides that are involved in interactions with cardiomyocytes have not been reported. Previously, in order to establish a DDS that targets the injured myocardium, we attempted to characterize a cell-surface lectin in cardiomyocytes by investigating the interaction of cardiomyocytes with glycosides. These interactions were examined by using a glycoside-adhesion assay, and the cardiomyocytes were incubated on various glycoside-bearing polymer-coated dishes. These glycoside-bearing polymers are composed of hydrophilic

* Corresponding author. Tel.: +81 263 37 3352; fax: +81 263 37 2573.

E-mail address: ise@sch.md.shinshu-u.ac.jp (H. Ise).

carbohydrates, such as lactose, glucose, galactose, mannose, maltose (MA), and *N*-acetylglucosamine (GlcNAc), and a hydrophobic vinylbenzyl moiety, and they are designated as multivalent glycoside ligands. These polymers adhere strongly to polystyrene dishes due to their amphiphilic property [9–11]. Cardiomyocytes adhered strongly to the GlcNAc-bearing polymer-coated dish but not to other glycoside-bearing polymer-coated dishes. From this result, we have found that cardiomyocytes exhibit a high degree of interactivity with GlcNAc and have also postulated that cardiomyocytes express a GlcNAc-recognizing lectin on their cell surface (unpublished data).

In this study, the specific uptake of GlcNAc-conjugated liposomes (GlcNAc-Ls) by cardiomyocytes was examined. GlcNAc-Ls and MA-conjugated liposomes (MA-Ls) were prepared by the post-insertion of GlcNAc- and MA-bearing polymers that are covalently linked to alkyl chains into the membrane of normal liposomes containing a fluorescence substrate or agent (Figs. 1 and 2) [12,13]. In order to circumvent their amphiphilic property and easily insert the glycoside-bearing polymers into the liposomal membranes, the

polymers were covalently linked to alkyl chains. Furthermore, we confirmed whether the agents encapsulated in GlcNAc-Ls are taken up by cardiomyocytes and whether they affect the intracellular environment of cardiomyocytes. We prepared glycoside-conjugated liposomes containing pravastatin. Pravastatin is a 3-hydroxy-3-methylglutaryl-CoA reductase inhibitor (statin) and is hydrophilic. Due to its hydrophilic nature, the intracellular uptake of pravastatin by cardiomyocytes is difficult [14,15]. In fact, we have previously reported that lipophilic statins and not the hydrophilic statin pravastatin augment inducible nitric oxide synthase (iNOS) expression and significantly increase nitric oxide (NO) production in interleukin-1 β (IL-1 β)-stimulated cardiomyocytes *via* the inhibition of small G proteins such as Ras and Rho GTP-binding proteins [14,15]. In the present study, we examined whether the uptake of GlcNAc-Ls-encapsulated pravastatin by cardiomyocytes augments iNOS expression and NO production in IL-1 β -stimulated cardiomyocytes. We found that cardiomyocytes interact with GlcNAc-Ls, and we achieved the effective uptake of agents by cardiomyocytes by encapsulating them in GlcNAc-Ls.

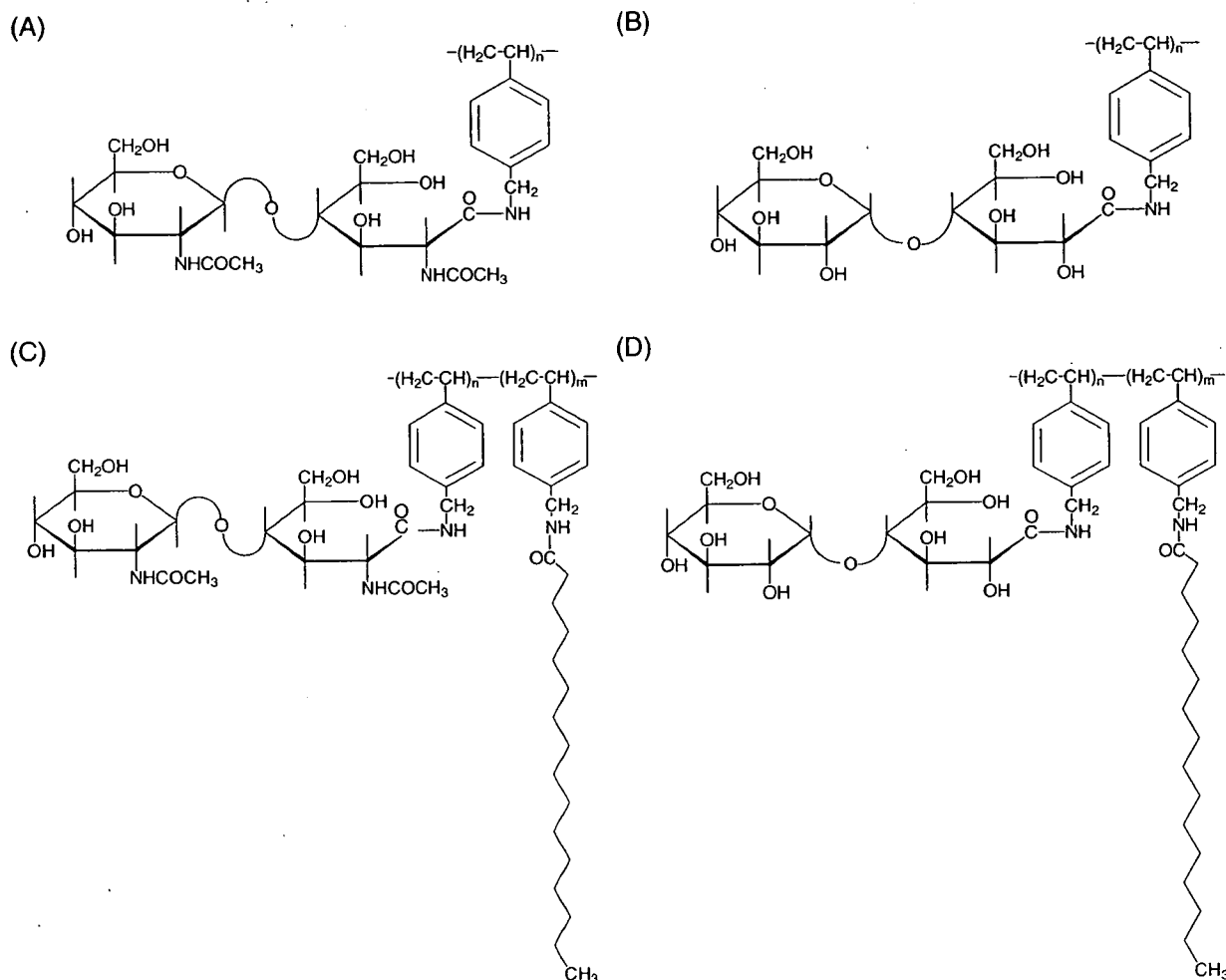


Fig. 1. Structure of PV-GlcNAc (A), PV-MA (B), P(VGlcNAc-co-1% and 5% VAL) (C), and P(VMA-co-5% VAL) (D). C: P(VGlcNAc-co-1% VAL), $n:m=99:1$; P(VGlcNAc-co-5% VAL), $n:m=95:5$. D: P(VMA-co-5% VAL), $n:m=95:5$.

2. Materials and methods

2.1. Materials

The glycoside-bearing polymers poly[*N-p*-vinylbenzyl-*O*-2-acetoamide-2-deoxy- β -D-glucopyranosyl-(1 \rightarrow 4)-2-acetoamide-2-deoxy- β -D-gluconamide] (PV-GlcNAc) and poly[*N-p*-vinylbenzyl-*O*- α -D-glucopyranosyl-(1 \rightarrow 4)-D-gluconamide] (PV-MA) were purchased from Celagix Research Ltd. (Yokohama, Japan). PV-GlcNAc and PV-MA are composed of a vinylbenzyl moiety and either chitobiose (GlcNAc terminal) or maltose (glucose terminal) (Fig. 1A and B) [9–11]. Three types of glycoside-bearing polymers covalently linked to alkyl chains, namely, P(VGlcNAc-co-1% 4-vinylbenzylhexadecanamide), P(VGlcNAc-co-1% VAL); P(VGlcNAc-co-5% 4-vinylbenzylhexadecanamide), P(VGlcNAc-co-5% VAL); and P(VMA-co-4-vinylbenzylhexadecanamide), P(VMA-co-5% VAL), were kindly provided by Celagix Research Ltd. P(VGlcNAc-co-1% VAL) is a low lipophilic polymer and is composed of 1% 4-vinylbenzylhexadecanamide and 99% chitobiose (Fig. 1C). P(VGlcNAc-co-5% VAL) is a high lipophilic polymer and is composed of 5% 4-vinylbenzylhexadecanamide and 95% chitobiose (Fig. 1C). P(VMA-co-5% VAL) is composed of 5% 4-vinylbenzylhexadecanamide and 95% maltose (Fig. 1D). P(VGlcNAc-co-1% VAL) differs from P(VGlcNAc-co-5% VAL)

in terms of the hydrophobicity of PV-GlcNAc, which is involved in its insertion into the liposome membranes. The preparation of these polymers was described previously [9–11]. Dipalmitoyl phosphatidylcholine (DPPC) and dipalmitoyl phosphatidylethanolamine (DPPE) were purchased from NOF Corporation (Tokyo, Japan). Cholesterol (Chol) and collagenase were purchased from Wako Pure Chemical Industries (Osaka, Japan). 1,1'-Dioctadecyl-3,3,3',3'-tetramethyl-indocarbocyanine perchlorate (DiI) and a cell detachment solution were purchased from Invitrogen Corp. (Carlsbad, CA, USA). Pravastatin was kindly provided by Sankyo Co., Ltd. (Tokyo, Japan). Pitavastatin was kindly provided by Kowa Co., Ltd. (Nagoya, Japan). Dulbecco's modified minimal essential medium (DMEM) and mouse monoclonal anti- β -actin antibodies were obtained from Sigma (St. Louis, MO, USA). Fetal bovine serum (FBS) was purchased from Equitech-Bio, Inc. (Kerrville, TX, USA). A protease inhibitor cocktail was purchased from Nacalai Tesque (Kyoto, Japan). Accutase was purchased from Innovative Cell Technologies, Inc. (La Jolla, CA, USA). Mouse monoclonal anti-iNOS antibodies were purchased from Becton, Dickinson and Company (BD) (Franklin Lakes, NJ, USA). Horseradish peroxidase (HRP)-conjugated rabbit anti-mouse IgG was purchased from Jackson ImmunoResearch Laboratories, Inc. (West Grove, PA, USA). All other chemicals were commercial products of analytical grade and purity.

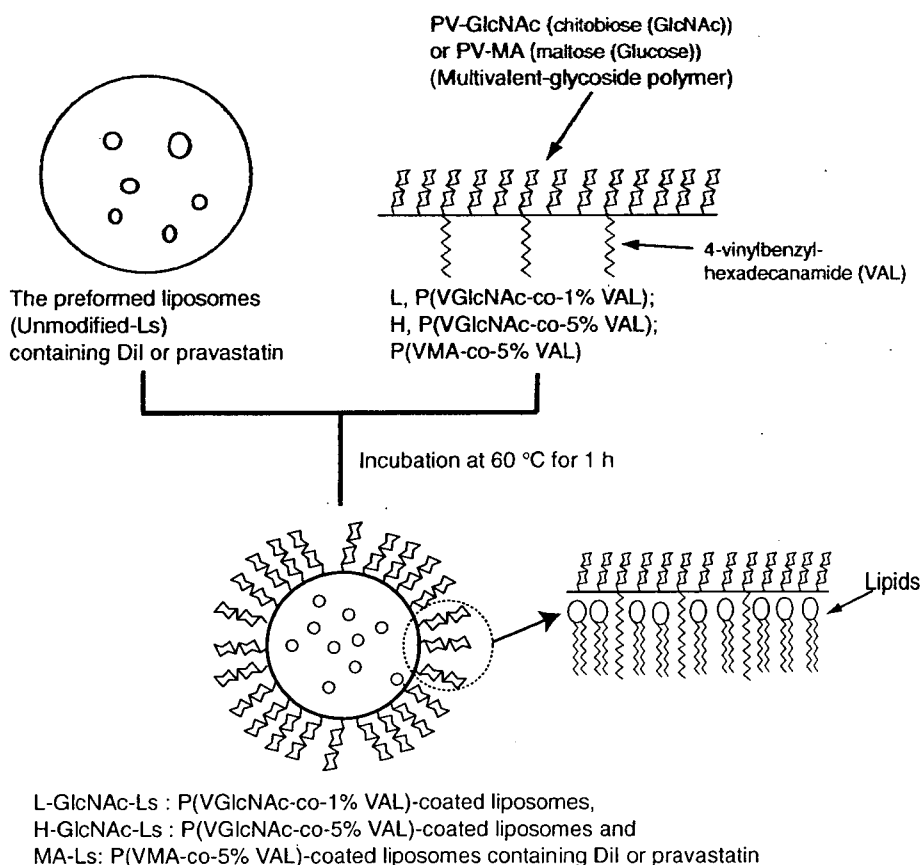


Fig. 2. Procedure of preparation of L-GlcNAc-Ls, H-GlcNAc-Ls, and MA-Ls by post-insertion of P(VGlcNAc-co-1% VAL), P(VGlcNAc-co-5% VAL), and P(VMA-co-5% VAL) into the preformed liposomes (unmodified-Ls).

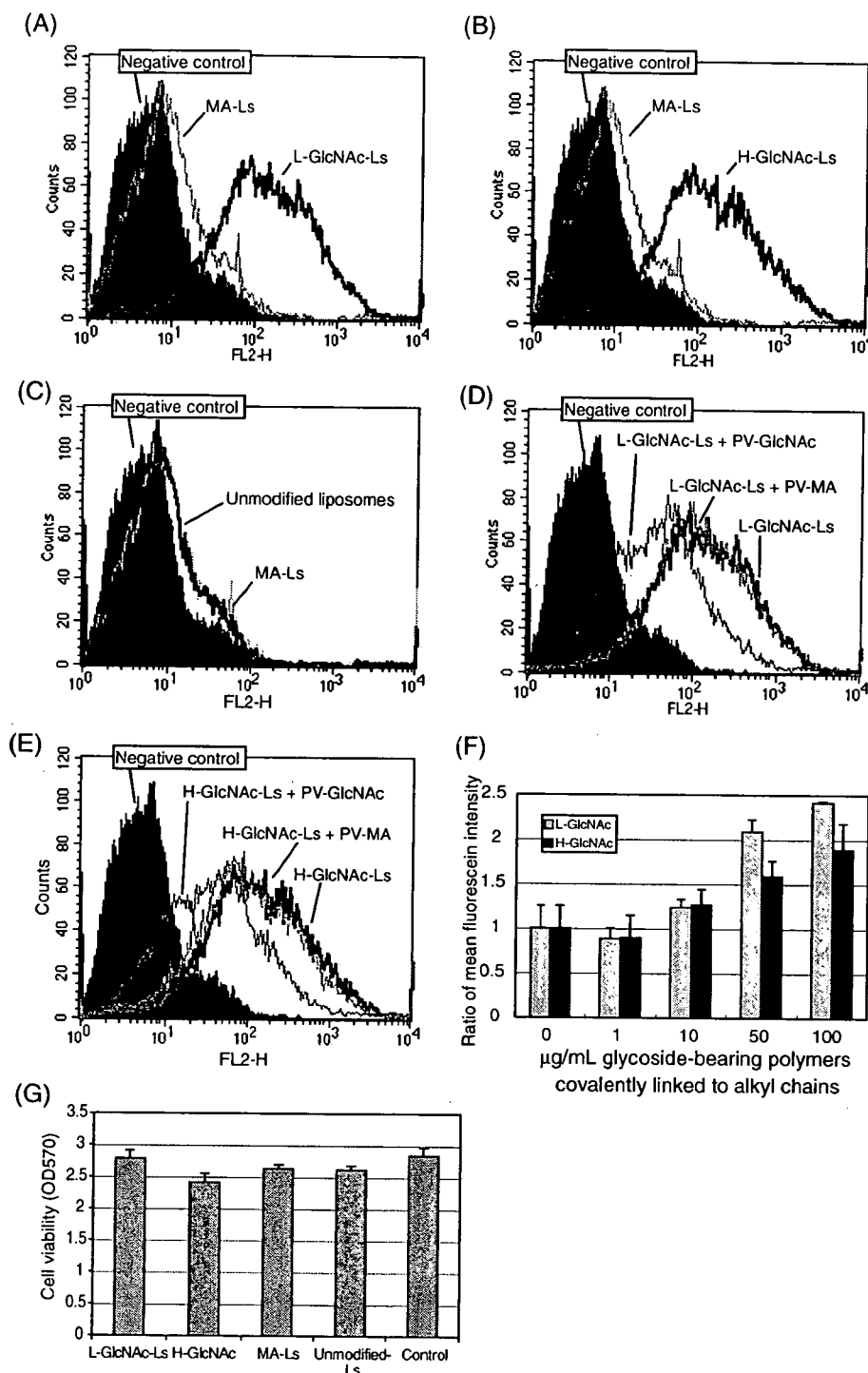


Fig. 3. Flow cytometric analysis of the interaction of L-GlcNAc-Ls, H-GlcNAc-Ls, and MA-Ls containing Dil with cardiomyocytes and the viability of cardiomyocytes. A: Comparison between L-GlcNAc-Ls and MA-Ls. B: Comparison between H-GlcNAc-Ls and MA-Ls. C: Comparison between unmodified-Ls and MA-Ls. D and E: Inhibition of the interaction of L- and H-GlcNAc-Ls into cardiomyocytes by 50 μg/mL PV-GlcNAc or PV-MA. F: The ratio of the mean fluorescein intensity of the interaction between 0–100 μg/mL P(VGlcNAc-co-1% VAL) (L-GlcNAc-Ls) and P(VGlcNAc-co-5% VAL) (H-GlcNAc-Ls) and cardiomyocytes. G: The effect of liposomes on cardiomyocyte viability. Cell viability was evaluated by the MTT assay. Cardiomyocytes were cultured in media (500 μL/well) in 24-well plates and incubated with 50 μL of each Dil-containing liposome solution (1.275 μmol lipids) for 24 h.

2.2. Cell culture

Cardiomyocytes were isolated by trypsin and collagenase digestion from the ventricles of 1-day-old Sprague–Dawley rats as described previously [14,15]. The rat cardiomyocytes

(6.25×10^4 cells/cm²) were cultured in DMEM supplemented with 10% FBS for 96 h at 37 °C in 95% air/5% CO₂. The cardiomyocytes were detached using accutase and the cell detachment solution, and the detached cells were washed and suspended in phosphate-buffered saline (PBS).

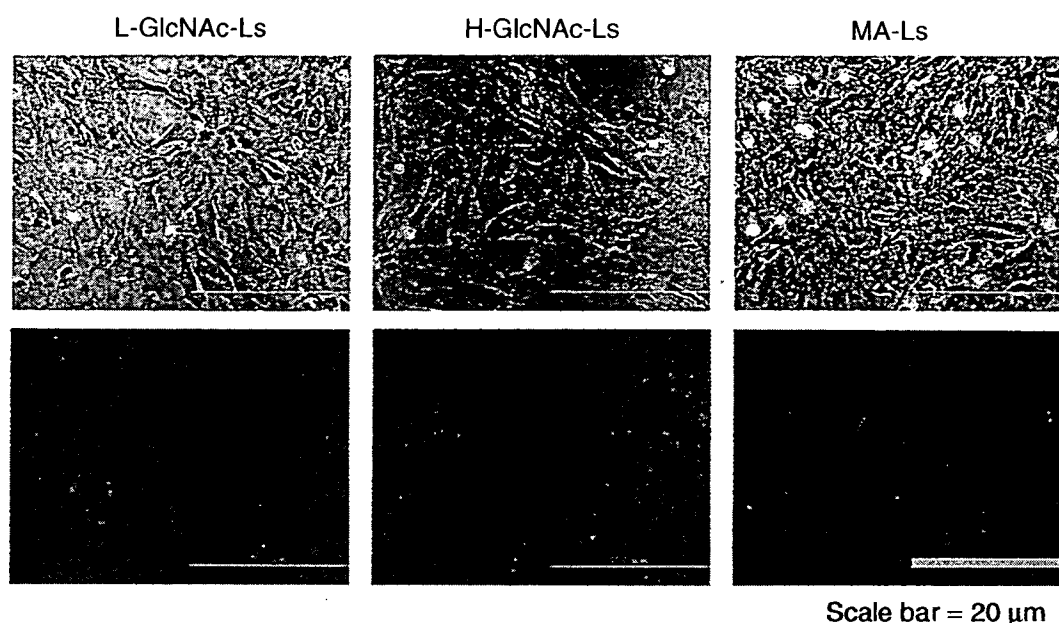


Fig. 4. Fluorescence microscopy images of the uptake of L-GlcNAc-Ls, H-GlcNAc-Ls, and MA-Ls containing DiI by cardiomyocytes. The upper panels show phase-contrast images, and the lower panels show fluorescence images. Magnification is $\times 200$. Scale bar = 20 μm .

2.3. Preparation of glycoside-conjugated liposomes containing DiI or pravastatin

Liposomes were prepared as previously described [12,13]. The liposomes were composed of DPPC:DPPE:Chol (80:2:20, molar ratio). When the liposomes were labeled with a fluorescence substrate, DiI was added to the lipid mixture at a ratio of 0.1 mol% to the total lipids. The lipids (80 μmol of DPPC, 20 μmol of Chol, and 2 μmol of DPPE) were dissolved in 5 mL of chloroform:methanol (7:3), and a lipid film was prepared by rotary evaporation. The lipid film was hydrated in 1 mL of PBS using a bath sonicator and a tip sonicator (Branson Ultrasonics Corporation, Danbury, CT, USA) with an output of 10 W for 10 min at 60 $^{\circ}\text{C}$ above the phase transition temperature; the resulting liposomes with a diameter of more than 0.45 μm were excluded by extrusion through polycarbonate membranes with a pore size of 0.45 μm . Pravastatin was encapsulated by hydrating the lipid film (102 μmol) with 1 mL of PBS containing 100 mM pravastatin, and the hydrated lipid suspension was frozen and thawed 3 times in order to increase the encapsulation of pravastatin into the liposomes. Unencapsulated pravastatin was removed from the suspension of liposomes containing pravastatin by centrifugation at 35,000 $\times g$ for 10 min. Finally, each liposome (25.5 μmol of lipids) was suspended in 1 mL of PBS. The conjugation of glycoside chains to these preformed liposomes containing DiI or pravastatin was performed by the post-insertion of P(VGlcNAc-co-1% or 5% VAL) or P(VMA-co-5% VAL). Two types of liposomes, namely, low lipophilic polymer- and high lipophilic polymer-GlcNAc-conjugated liposomes (L-GlcNAc-Ls and H-GlcNAc-Ls, respectively), were prepared by mixing 100 $\mu\text{g}/\text{mL}$ P(VGlcNAc-co-1% VAL) and P(VGlcNAc-co-5% VAL), respectively, with the preformed liposomes (25.5 μmol of lipids)

for 1 h at 60 $^{\circ}\text{C}$ (Fig. 2). MA-Ls were prepared by mixing 100 $\mu\text{g}/\text{mL}$ P(VMA-co-5% VAL) with the preformed liposomes (25.5 μmol of lipids) for 1 h at 60 $^{\circ}\text{C}$ (Fig. 2). The preformed liposomes (unmodified-Ls) were prepared as nontargeted control liposomes. Moreover, to estimate the amounts of glycoside-bearing polymers in the liposomal surface, liposomes containing DiI that 0, 1, 10, 50, and 100 $\mu\text{g}/\text{mL}$ P(VGlcNAc-co-1% or 5% VAL) were post-inserted into were prepared. The amounts of glycoside-bearing polymers in the liposomes were estimated from the interaction of these liposomes with cardiomyocytes. The particle sizes of these liposomes were measured in a dynamic light scattering spectrophotometer (Zetasizer, Sysmex corporation, Tokyo, Japan). The cytotoxicity of these liposomes was evaluated in cardiomyocytes by a 3-(4,5-dimethylthiazol-2-yl)-2,5-diphenyltetrazolium bromide (MTT) assay (Nacalai Tesque, Kyoto, Japan). The cardiomyocytes were cultured in media (500 $\mu\text{L}/\text{well}$) in 24-well plates and incubated with 50 μL of each DiI-containing liposome solution (1.275 μmol lipids) for 24 h. At 24 h after incubation, 50 μL of the 5 mg/mL MTT solution was added to each well, and the cells were incubated for another 2 h. MTT formazan, regarded as an indicator of cell viability, was quantified

Table 1
Particle size distributions of liposomes prepared by sonication

Liposomes	Particle size (nm) in diameter
L-GlcNAc-Ls	140 \pm 21.0
H-GlcNAc-Ls	119 \pm 14.9
MA-Ls	145 \pm 21.9
Unmodified-Ls	149 \pm 27.1

Values represent means \pm S.D.

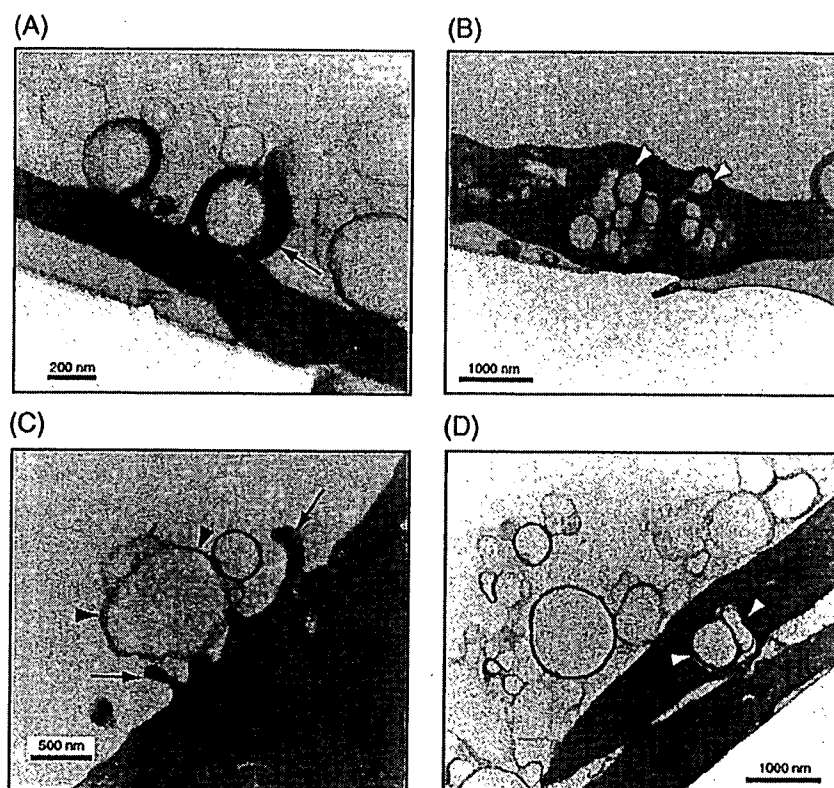


Fig. 5. Electron microscopy images of the uptake of GlcNAc-Ls by cardiomyocytes. A and B: The incubation of 0.4- μm -sized H-GlcNAc-Ls with cardiomyocytes. C and D: The incubation of 0.8- μm -sized H-GlcNAc-Ls with cardiomyocytes. A and C: Black arrowheads show the liposomes internalized by cardiomyocytes and arrows show the microvilli of the cardiomyocytes (A: $\times 12,000$ and C: $\times 10,000$). B and D: White arrowheads show the liposomes internalized by the cardiomyocytes ($\times 8000$).

colorimetrically. The absorbance at 570 nm was determined using a microplate reader (Bio-Rad, Richmond, CA, USA).

To examine the endocytic capacity of cardiomyocytes for GlcNAc-Ls, H-GlcNAc-Ls of 2 different sizes were prepared by extrusion of the hydrated lipid suspension through 0.4- or 0.8- μm polycarbonate membrane filters by using an extruder (Avanti polar lipids, Inc., AL, USA). The 0.4- or 0.8- μm -sized H-GlcNAc-Ls were prepared by post-insertion of 100 $\mu\text{g}/\text{mL}$ P (VGlcNAc-co-5% VAL). The uptake of 0.4- or 0.8- μm -sized H-GlcNAc-Ls by the cardiomyocytes was observed by transmission electron microscopy.

L-GlcNAc-Ls, H-GlcNAc-Ls, MA-Ls, or unmodified-Ls-containing DiI or pravastatin were prepared by sonication of the hydrated lipid suspension, and the liposomes with a diameter of more than 0.45 μm were excluded; 0.4- or 0.8- μm -sized H-GlcNAc-Ls were prepared by repeated extrusion through 0.4- or 0.8- μm polycarbonate membrane filters by using an extruder.

2.4. Flow cytometric analysis of interaction of the liposomes containing DiI with cardiomyocytes

The interaction of 0, 1, 10, 50, or 100 $\mu\text{g}/\text{mL}$ P(VGlcNAc-co-1% or 5% VAL)-post-inserted liposomes (L-GlcNAc-Ls or H-GlcNAc-Ls), MA-Ls, or unmodified-Ls-containing DiI with cardiomyocytes were analyzed by flow cytometry. The detached cells were suspended in PBS containing 1% bovine

serum albumin, and 1 mL of the cell suspension was incubated with each liposome (1.275 μmol lipids) for 1 h at 37 $^{\circ}\text{C}$. After the incubation period, the cells were washed and resuspended in PBS. Flow cytometric analysis was performed using a FACS Calibur (BD, NJ, USA).

2.5. Fluorescence microscopy analysis of the uptake of liposomes by cardiomyocytes

The cardiomyocytes cultured in 3.5-cm dishes were incubated with each liposome (1.275 μmol lipids) for 1 h at 37 $^{\circ}\text{C}$. After the incubation period, the cells were washed repeatedly in PBS and observed by fluorescence microscopy (Olympus Corp., Tokyo, Japan).

2.6. Electron microscopy analysis of the uptake of GlcNAc-Ls by cardiomyocytes

The cardiomyocytes were cultured on 24-mm glass coverslips. The cells were incubated with 0.4- or 0.8- μm -sized H-GlcNAc-Ls for 2 h at 37 $^{\circ}\text{C}$. The cells were fixed with 2.5% glutaraldehyde at 4 $^{\circ}\text{C}$ overnight. After washing with phosphate buffer (PB), the cells were fixed with 1% osmium tetroxide in PB for 20 min and then fixed with 2% tannin/2.5% glutaraldehyde for 20 min and further fixed with 1% osmium tetroxide in PB for 20 min at 4 $^{\circ}\text{C}$. The cells were then serially dehydrated in ethanol and embedded in Epon

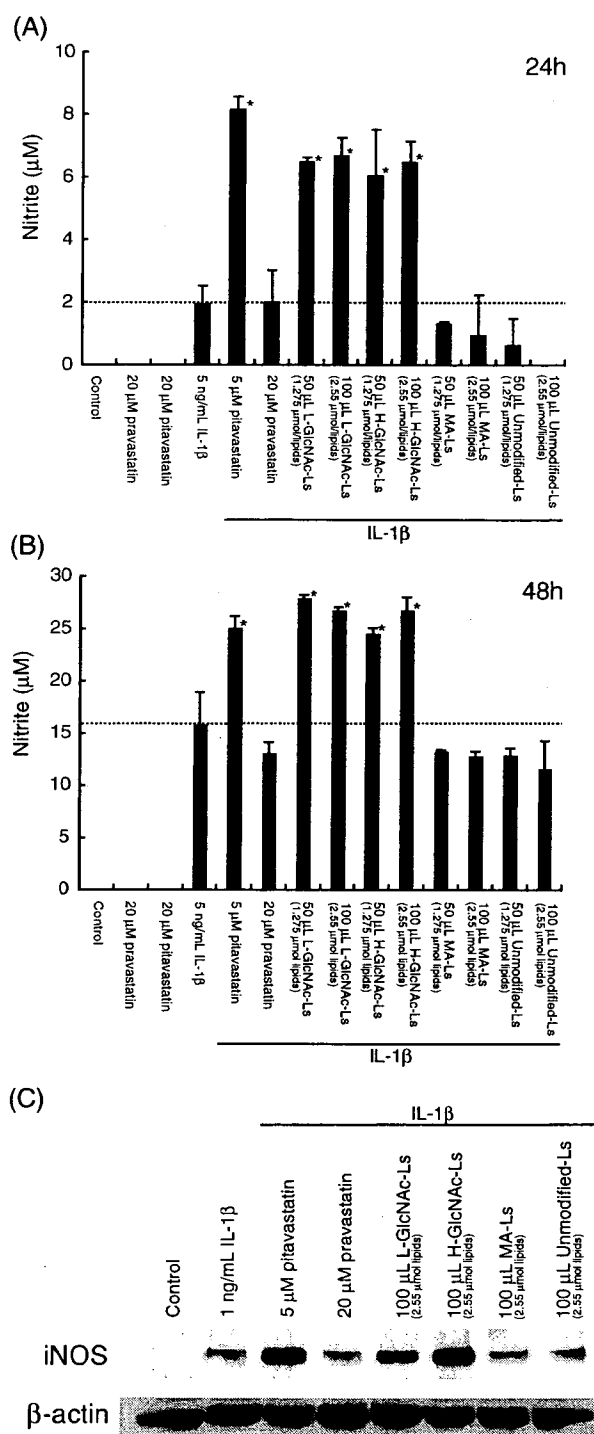


Fig. 6. NO production and iNOS expression, following the uptake of L-GlcNAc-Ls, H-GlcNAc-Ls, MA-Ls, and unmodified-Ls-containing pravastatin, pravastatin, and pitavastatin in 5-ng/mL and 1-ng/mL IL-1 β -stimulated cardiomyocytes. A and B: NO production in 5-ng/mL IL-1 β -stimulated cardiomyocytes at 24 and 48 h. * p < 0.05, when compared with other samples. C: iNOS and β -actin expression in 1-ng/mL IL-1 β -stimulated cardiomyocytes at 24 h; the iNOS protein (130 kDa) and β -actin (42 kDa) were detected by western blotting.

812 for polymerization at 60 °C overnight. The embedded cells were thin-sectioned, and these sections of 100-nm thickness were placed on copper grids that were double-stained with uranyl acetate and lead citrate. These sections

were examined with a JEOL 1200EX transmission electron microscope.

2.7. Measurement of the concentration of pravastatin encapsulated in L-GlcNAc-Ls, H-GlcNAc-Ls, MA-Ls, and unmodified-Ls

Pravastatin encapsulated in each liposome (1.275 μ mol lipids) was obtained by the dissolution of the liposome in methanol and was quantified colorimetrically. The absorbance of pravastatin at 239 nm was determined using a colorimeter (GE Healthcare Bio-Sciences Corp., Piscataway, NJ, USA). The pravastatin concentrations were calculated by comparison with the absorbance of the standard solutions of pravastatin prepared in methanol.

2.8. Measurement of NO

The cardiomyocytes were cultured in 12-well plates. At 1 h after the addition of various liposomes containing pravastatin as the hydrophilic statin, pravastatin, or pitavastatin as the lipophilic statin, the cardiomyocytes were treated with IL-1 β at a concentration of 5 ng/mL. At 24 or 48 h after the treatment with IL-1 β , nitrite accumulation—an indicator of NO production—was measured in the conditioned medium. Nitrite was quantified colorimetrically after adding 100 μ L of Griess reagent (1% sulfanilamide and 0.1% naphthylendiamine in 5% phosphoric acid) to 100 μ L samples. The absorbance at 540 nm was determined using a microplate reader (Bio-Rad, Richmond, CA, USA). The nitrite concentrations were calculated by comparison with the absorbance of standard solutions of sodium nitrite prepared in the culture medium.

2.9. Estimation of iNOS by western blotting

The cardiomyocytes were cultured in 3.5-cm dishes. At 24 h after the treatment of 1-ng/mL IL-1 β -stimulated cardiomyocytes with various liposomes containing pravastatin as the hydrophilic statin, pravastatin, or pitavastatin as the lipophilic statin, these cells were lysed using radioimmunoprecipitation assay (RIPA) buffer (25 mM Tris-HCl, 2.5 mM ethylenediaminetetraacetic acid, 137 mM NaCl, 1% sodium deoxycholic acid, 0.1% sodium dodecylsulfate [SDS], 1% Triton X-100, 2 mM phenylmethyl sulfonyl fluoride, and protease inhibitor cocktail). The protein concentrations of the samples were measured by the Bio-Rad DC protein assay. The samples were resolved by electrophoresis on a 7.5% SDS-polyacrylamide gel under reducing conditions and were transferred to polyvinylidene difluoride membranes (Bio-Rad). Subsequently, the membranes were incubated with mouse monoclonal anti-iNOS antibodies (1:2500) or mouse monoclonal anti- β -actin antibodies (1:10,000) as the primary antibodies, followed by incubation with HRP-anti-mouse IgG antibodies (1:20,000) as the secondary antibodies. The membranes were developed using Immobilon Western Detection Reagents (Millipore Corp., Billerica, MA, USA) according to the manufacturer's instructions.

Table 2
The amount of pravastatin encapsulated in various liposomes

Liposomes	nmol/mmol lipids
L-GlcNAc-Ls	0.498±0.14
H-GlcNAc-Ls	0.457±0.06
MA-Ls	0.478±0.07
Unmodified-Ls	0.380±0.06

Values represent means±S.D.; $p>0.1$, L-GlcNAc-Ls or H-GlcNAc-Ls versus MA-Ls or unmodified-Ls.

2.10. Statistical analysis

All data are expressed as mean±S.D., and the statistical analyses of the 2 groups were performed using the unpaired Student's *t* test. A probability (*p*) value of <0.05 was considered to be statistically significant.

3. Results

3.1. Cardiomyocytes interact with GlcNAc-Ls

To investigate whether glycoside chains interact with cardiomyocytes, the interaction of L-GlcNAc-Ls (100 µg/mL P(VGlcNAc-co-1% VAL)), H-GlcNAc-Ls (100 µg/mL P(VGlcNAc-co-5% VAL)), MA-Ls (100 µg/mL P(VMA-co-5% VAL)), or unmodified-Ls-containing DiI with cardiomyocytes was analyzed by flow cytometry. L- and H-GlcNAc-Ls were adequately taken up by cardiomyocytes whereas both MA-Ls and unmodified-Ls were scarcely taken up (Fig. 3A, B, and C). Moreover, the binding of L- and H-GlcNAc-Ls to cardiomyocytes was inhibited by the soluble PV-GlcNAc but not by the soluble PV-MA (Fig. 3D and E). The degree of interaction increased with an increase in the addition of 0–100 µg/mL P(VGlcNAc-co-1% or 5% VAL) to the preformed liposomes containing DiI (Fig. 3F). The interaction of L-GlcNAc-Ls and H-GlcNAc with the cardiomyocytes was almost saturated with the addition of 100 µg/mL P(VGlcNAc-co-1% or 5% VAL) to the liposomes. From these results, we assumed that 100 µg/mL P(VGlcNAc-co-1% or 5% VAL) was almost adsorbed on the surface of the liposomes and estimated that the amount of this post-inserted polymer into L-GlcNAc-Ls and H-GlcNAc-Ls was 3.9 µg P(VGlcNAc-co-1% or 5% VAL)/µmol lipids. The densities of the ligands on the surface of these liposomes were estimated to be approximately 0.7 mol% of the ligands of the liposomal lipids, because the molecular weight of GlcNAc-ligand monomer of P(VGlcNAc-co-1% VAL) and P(VGlcNAc-co-5% VAL) is 557. Furthermore, we assumed that the amount of post-inserted 100 µg/mL P(VMA-co-5% VAL) into MA-Ls was similar. The polymer did not have cytotoxicity because these liposomes did not affect the cell viability at 24 h (Fig. 3G). Fig. 4 shows that L- and H-GlcNAc-Ls were adequately taken up by the cultured cardiomyocytes whereas MA-Ls were scarcely taken up. We suggested that both L- and H-GlcNAc-Ls were efficiently internalized by cardiomyocytes. These liposomes were prepared by sonicating the lipid film, and the liposomes with a diameter greater than 0.45 µm were excluded by 0.45-µm polycarbonate membranes; therefore, the particle

sizes of L- and H-GlcNAc-Ls, MA-Ls, and unmodified-Ls were analyzed by a dynamic light scattering spectrophotometer and were approximately 140 nm (Table 1).

Next, to examine the endocytic capacity of cardiomyocytes for GlcNAc-Ls, we observed the uptake of 0.4- and 0.8-µm-sized H-GlcNAc-Ls by the cardiomyocytes by transmission electron microscopy. Fig. 5A and C shows the instant when the 0.4 and 0.8 µm-sized H-GlcNAc-Ls were internalized by cardiomyocytes. Fig. 5B and D show that these GlcNAc-Ls accumulated in cardiomyocytes. These results show that cardiomyocytes at least have the endocytic capacity for 0.8-µm-sized GlcNAc-Ls.

These results show that GlcNAc-Ls interact with cardiomyocytes through GlcNAc; hence, cardiomyocytes exhibit a high degree of interaction with GlcNAc-Ls.

3.2. NO production by IL-1β-stimulated cardiomyocytes was enhanced by GlcNAc-Ls-containing pravastatin

We examined whether the hydrophilic statin pravastatin enters cardiomyocytes by using GlcNAc-Ls. The lipophilic statin pitavastatin significantly increased IL-1β-induced NO production by cardiomyocytes; however, a similar result was not observed for the hydrophilic statin pravastatin because it was scarcely taken up by the cells (Fig. 6A and B). L- and H-GlcNAc-Ls-containing pravastatin increased NO production by IL-1β-stimulated cardiomyocytes to a similar extent; however, MA-Ls- and unmodified-Ls-containing pravastatin did not increase NO production (Fig. 6A and B). There was no significant difference in the amount of pravastatin encapsulated in L-GlcNAc-Ls, H-GlcNAc-Ls, MA-Ls, and unmodified-Ls but that in the unmodified-Ls was slightly low as compared with that in L-GlcNAc-Ls, H-GlcNAc-Ls, and MA-Ls. The encapsulation efficiency of these liposomes was very low (Table 2). The enhancement of NO production by 50 µL (1.275 µmol lipids) of GlcNAc-Ls-containing pravastatin (approximately 0.6 nmol pravastatin) was equal to the increase in NO production by 5 nmol of lipophilic pitavastatin (5 µM pitavastatin) in 1 mL of culture medium. These results show that the encapsulation of pravastatin in GlcNAc-Ls has a considerable effect on cardiomyocytes.

3.3. iNOS expression by IL-1β-stimulated cardiomyocytes was enhanced by GlcNAc-Ls-containing pravastatin

We examined whether iNOS expression in IL-1β-stimulated cardiomyocytes was enhanced by treatment with GlcNAc-Ls-containing pravastatin. The iNOS expression was assayed by western blotting. The expression of iNOS in cardiomyocytes was enhanced by both GlcNAc-Ls-containing pravastatin but not by the MA-Ls- and unmodified-Ls-containing pravastatin (Fig. 6C). The increase in NO production by both the GlcNAc-Ls was accompanied with increased iNOS expression.

4. Discussion

In the present study, we demonstrated that cardiomyocytes exhibit a high degree of interactivity with GlcNAc-Ls and that

agents encapsulated in GlcNAc-Ls could be effectively taken up by cardiomyocytes. We believed that the amphiphilic property of a glycoside-bearing polymer covalently linked to alkyl chains can affect its insertion into and the perturbation of liposomes [12]; hence, we examined the post-insertion of 2 types of glycoside-bearing polymers—P(VGlcNAc-co-1% VAL) and P(VGlcNAc-co-5% VAL)—into preformed liposomes. The amounts of pravastatin encapsulated in L-GlcNAc-Ls, H-GlcNAc-Ls, MA-Ls, and unmodified-Ls were almost similar; furthermore, since both L- and H-GlcNAc-Ls were taken up by cardiomyocytes at a similar level, we estimated that both P(VGlcNAc-co-1% VAL) and P(VGlcNAc-co-5% VAL) were inserted in a similar manner into the surface of the preformed liposomes. These findings indicate that the liposomes were firmly formed by the post-insertion procedure.

Cell-specific targeting systems for the delivery of agents have been developed using glycosylated macromolecules as a vehicle that can be selectively recognized by cell-surface lectins. Many delivery systems using glycosylated carriers have been developed, and their usefulness has been investigated in various settings [4,5,8,16,17]. Liver-targeted DDSs are well-established delivery systems because the liver cells possess a galactose-binding protein known as hepatic asialoglycoprotein receptor [18,19]. This receptor that exists on the surface of hepatocytes plays a role in receptor-mediated endocytosis and binds to galactose/*N*-acetylgalactosamine-terminated ligands [19–21]. In order to obtain a liver-specific DDS, galactose-conjugated liposomes containing agents and genes, and desialylated bone marrow cells were developed [22–25]. The targeting of transcription factors such as nuclear factor- κ B decoy complexes to liver nonparenchymal cells by using mannose- and hyaluronic acid-conjugated polymers significantly prevented liver failure because Kupffer cells and liver sinusoidal endothelial cells are known to express a large number of mannose receptors and unique receptors that recognize and internalize hyaluronic acid, respectively, on their surface [16,17]. Cell-specific targeting systems for the delivery of agents are well established for tissues in which cell-surface lectins have been elucidated. Hence, the identification of cell-surface lectins in the myocardium can facilitate the establishment of a myocardium-targeted DDS. It is reported that positively charged liposomes were taken up by cultured cardiomyocytes [26,27], and the uptake of hemagglutinating virus of Japan (HVJ)-liposomes containing nuclear factor- κ B decoy complexes by cardiomyocytes suppressed cardiac inflammation [28]. However, in our study, unmodified liposomes and MA-Ls were not taken up by cardiomyocytes. We consider that positively charged and HVJ liposomes might be internalized by cardiomyocytes nonspecifically.

In the present study, we found that the binding of GlcNAc-Ls to cardiomyocytes through specific interaction with GlcNAc is not dependent on temperature (data not shown). Previously, we have also found that cardiomyocytes adhered strongly to GlcNAc-bearing polymer-coated dishes (data not shown). Moreover, the internalization of 0.4- and 0.8- μ m-sized GlcNAc-Ls into cardiomyocytes, and the enhancement of NO production and iNOS expression in cardiomyocytes by GlcNAc-

Ls-encapsulated pravastatin indicate that GlcNAc-Ls were endocytosed into cardiomyocytes and the encapsulated pravastatin affected the intracellular environment of cardiomyocytes. We observed that cardiomyocytes internalized 0.4- and 0.8- μ m-sized GlcNAc-Ls by microvilli. It is known that the binding of lectins to carbohydrates is not temperature dependent and that cell-surface lectins possess the property of internalizing lectin-bound carbohydrates [4,6,19]. Based on these results, we suggest that cardiomyocytes probably express a lectin-recognizing GlcNAc, *i.e.*, a GlcNAc-binding protein, on the cell surface. It is reported that GlcNAc-binding cell-surface lectins are expressed on airway epithelial cells [29]. Although these GlcNAc-binding cell-surface lectins remain to be determined, the GlcNAc-binding protein on cardiomyocytes might be similar to that on airway epithelial cells. Thus, further investigations are required to elucidate the GlcNAc-binding protein.

In order to establish a DDS using the GlcNAc-binding protein, the expression of this protein in another tissue should be investigated. Although this issue remains to be studied, we assume that endothelial cells may not considerably express the GlcNAc-binding protein under unactivated conditions because unactivated human umbilical vein endothelial cells weakly interact with GlcNAc-Ls (data not shown); further, the accumulation of intravenously injected GlcNAc-bearing liposomes has not been observed in any specific tissue [1,30]. In preliminary experiments, we systemically administered GlcNAc-conjugated fluorescein isothiocyanate (FITC)-polystyrene particles (200 nm) to a mouse model of myocardial ischemia-reperfusion. The accumulation of these particles was observed in the injured myocardium, spleen, and liver, but the accumulation of these particles was not observed in the uninjured myocardium and in other tissues (data not shown). We assume that the accumulation of these particles might be nonspecific in the spleen and liver. GlcNAc-Ls may similarly not interact with the normal myocardium *in vivo*; this is because the inner region of the vessels in the normal myocardium is covered with endothelial cells, thereby preventing the direct contact of these GlcNAc-Ls with cardiomyocytes. However, we postulate that GlcNAc-Ls could accumulate in the region of the injured myocardium because they would come in direct contact with cardiomyocytes due to the destruction of vessels induced by ischemia-reperfusion injury. Thus, further investigations are required to perform *in vivo* experiments by using GlcNAc-Ls.

In conclusion, it is expected that GlcNAc-Ls might be utilized for therapeutic applications such as catheterization involving the direct injection of agents into the region of the injured myocardium and gene transfection involving the treatment of cultured cardiomyocytes with encapsulated liposomes. Based on these results, we suggest that the development of a DDS using GlcNAc-Ls-encapsulated cardioprotective agents such as anti-apoptotic and anti-inflammatory agents might be a promising approach for the treatment of cardiovascular diseases.

Acknowledgments

We are grateful to Junko Nakayama, Tomoko Hamaji, and Kazuko Misawa for excellent technical assistance. This work was


supported in part by a Grant-in-aid for Scientific Research from the Ministry of Education, Science, Sports and Culture of Japan.

References

- [1] N. Yamazaki, S. Kojima, N.V. Bovin, S. Andre, S. Gabius, H.J. Gabius, Endogenous lectins as targets for drug delivery, *Adv. Drug Deliv. Rev.* 43 (2000) 225–244.
- [2] S.L. Hatt, R.P. Harbottle, R. Cooper, A. Miller, R. Williamson, C. Coutelle, Gene delivery and expression mediated by an integrin-binding peptide, *Gene Ther.* 2 (1995) 552–554.
- [3] G.A. Koning, R.M. Schiffelers, M.H. Wauben, R.J. Kok, E. Mastrobattista, G. Molema, T.L.M. ten Hagen, G. Storm, Targeting of angiogenic endothelial cells at sites of inflammation by dexamethasone phosphate-containing RGD peptide liposomes inhibits experimental arthritis, *Arthritis Rheum.* 54 (2006) 1198–1208.
- [4] M. Monsigny, A.C. Roche, P. Midoux, R. Mayer, Glycoconjugates as carriers for specific delivery of therapeutic drugs and genes, *Adv. Drug Deliv. Rev.* 14 (1994) 1–24.
- [5] M. Nishikawa, Development of cell-specific targeting system for drugs and genes, *Biol. Pharm. Bull.* 28 (2005) 195–200.
- [6] W.I. Weis, K. Drickamer, Structural basis of lectin–carbohydrate recognition, *Annu. Rev. Biochem.* 65 (1996) 441–473.
- [7] A.C. Roche, I. Fajac, S. Grosse, N. Frison, C. Rondanino, R. Mayer, M. Monsigny, Glycofection: facilitated gene transfer by cationic glycopolymers, *Cell. Mol. Life Sci.* 60 (2) (2003) 288–297.
- [8] S.E. Cook, I.K. Park, E.M. Kim, H.J. Jeong, T.G. Park, Y.J. Choi, T. Akaike, C.S. Cho, Galactosylated polyethylenimine-graft-poly(vinylpyrrolidone) as a hepatocyte-targeting gene carrier, *J. Control. Release* 105 (2005) 151–163.
- [9] K. Kobayashi, H. Sumimoto, Synthesis and functions of polystyrene derivatives having pendent oligosaccharides, *Polym. J.* 17 (1985) 567–575.
- [10] K. Kobayashi, H. Sumimoto, Y. Ina, A carbohydrate-containing synthetic polymer obtained from *N-p*-vinylbenzyl-D-gluconamid, *Polym. J.* 15 (1983) 667–671.
- [11] A. Maruyama, T. Ishihara, N. Adachi, T. Akaike, Preparation of nanoparticles bearing high density carbohydrate chains using carbohydrate-carrying polymers as emulsifier, *Biomaterials* 15 (1994) 1035–1042.
- [12] T. Ishida, D.L. Iden, T.M. Allen, A combinatorial approach to producing sterically stabilized (Stealth) immunoliposomal drugs, *FEBS Lett.* 460 (1999) 129–133.
- [13] S.J. Chiu, S. Liu, D. Perrotti, G. Marcucci, R.J. Lee, Efficient delivery of a Bcl-2-specific antisense oligodeoxyribonucleotide (G3139) via transferrin receptor-targeted liposomes, *J. Control. Release* 112 (2006) 199–207.
- [14] U. Ikeda, M. Shimpō, M. Ikeda, S. Minota, K. Shimada, Lipophilic statins augment inducible nitric oxide synthase expression in cytokine-stimulated cardiac myocytes, *J. Cardiovasc. Pharmacol.* 38 (2001) 69–77.
- [15] Y. Ogata, M. Takahashi, K. Takeuchi, S. Ueno, H. Mano, S. Ookawara, E. Kobayashi, U. Ikeda, K. Shimada, Fluvastatin induces apoptosis in rat neonatal cardiac myocytes: a possible mechanism of statin-attenuated cardiac hypertrophy, *J. Cardiovasc. Pharmacol.* 40 (2002) 907–915.
- [16] Y. Higuchi, S. Kawakami, M. Oka, Y. Yabe, F. Yamashita, M. Hashida, Intravenous administration of mannosylated cationic liposome/NF- κ B decoy complexes effectively prevent LPS-induced cytokine production in a murine liver failure model, *FEBS Lett.* 580 (2006) 3706–3714.
- [17] Y. Takei, A. Maruyama, A. Ferdous, Y. Nishimura, S. Kawano, K. Ikejima, S. Okumura, S. Asayama, M. Nogawa, M. Hashimoto, Y. Makino, M. Kinoshita, S. Watanabe, T. Akaike, J.J. Lemasters, N. Sato, Targeted gene delivery to sinusoidal endothelial cells: DNA nanoassociate bearing hyaluronan–glycocalyx, *FASEB J.* 18 (2004) 699–701.
- [18] G.Y. Wu, V. Keegan-Rogers, S. Franklin, S. Midford, C.H. Wu, Targeted antagonism of galactosamine toxicity in normal rat hepatocytes in vitro, *J. Biol. Chem.* 263 (1988) 4719–4723.
- [19] R.J. Stockert, The asialoglycoprotein receptor: relationships between structure, function, and expression, *Physiol. Rev.* 75 (1995) 591–609.
- [20] H. Ise, N. Sugihara, N. Negishi, T. Nikaido, T. Akaike, Low asialoglycoprotein receptor expression as markers for highly proliferative potential hepatocytes, *Biochem. Biophys. Res. Commun.* 285 (2001) 172–182.
- [21] H. Ise, T. Nikaido, N. Negishi, N. Sugihara, F. Suzuki, T. Akaike, U. Ikeda, Effective hepatocyte transplantation using rat hepatocytes with low asialoglycoprotein receptor expression, *Am. J. Pathol.* 165 (2004) 501–510.
- [22] T. Terada, M. Iwai, S. Kawakami, F. Yamashita, M. Hashida, Novel PEG-matrix metalloproteinase-2 cleavable peptide–lipid containing galactosylated liposomes for hepatocellular carcinoma-selective targeting, *J. Control. Release* 111 (2006) 333–342.
- [23] C. Diaz, E. Vargas, O. Gatjens-Boniche, Cytotoxic effect induced by retinoic acid loaded into galactosyl-sphingosine containing liposomes on human hepatoma cell lines, *Int. J. Pharm.* 325 (2006) 108–115.
- [24] Y. Aramaki, I. Lee, H. Arima, T. Sakamoto, Y. Magami, T. Yoshimoto, F. Moriyasu, J. Mizuguchi, Y. Koyanagi, T. Nikaido, S. Tsuchiya, Efficient gene transfer to hepatoblastoma cells through asialoglycoprotein receptor and expression under the control of the cyclin A promoter, *Biol. Pharm. Bull.* 26 (2003) 357–360.
- [25] R. Misawa, H. Ise, M. Takahashi, H. Morimoto, E. Kobayashi, S. Miyagawa, U. Ikeda, Development of liver regenerative therapy using glycoside-modified bone marrow cells, *Biochem. Biophys. Res. Commun.* 342 (2006) 434–440.
- [26] Y. Chen, Y.J. Deng, Y.L. Hao, A.J. Hao, H.J. Zhong, X.M. Wang, Uptake of liposomes by cultured cardiomyocytes, *Pharmazie* 60 (2005) 844–848.
- [27] Y. Chen, Y.J. Deng, Y.L. Hao, Surface modification of liposomes for cardiomyocytes targeting in vitro, *Pharmazie* 60 (2005) 238–240.
- [28] Y. Sawa, R. Morishita, K. Suzuki, K. Kagisaki, Y. Kaneda, K. Maeda, K. Kadoba, H. Matsuda, A novel strategy for myocardial protection using in vivo transfection of cis element ‘decoy’ against NF κ B binding site: evidence for a role of NF κ B in ischemia-reperfusion injury, *Circulation* 96 (1997) 280–285.
- [29] M.M. Issa, M. Koping-Hoggard, K. Tommeraa, K.M. Varum, B.E. Christensen, S.P. Strand, P. Artursson, Targeted gene delivery with trisaccharide-substituted chitosan oligomers in vitro and after lung administration in vivo, *J. Control. Release* 115 (2006) 103–112.
- [30] N. Yamazaki, S. Kojima, S. Gabius, H.J. Gabius, Studies on carbohydrate-binding proteins using liposome-based systems-I. Preparation of neoglycoprotein-conjugated liposomes and the feasibility of their use as drug-targeting devices, *Int. J. Biochem.* 24 (1992) 99–104.

Circulation Research

JOURNAL OF THE AMERICAN HEART ASSOCIATION

American Heart
Association® 
Learn and Livesm

Interleukin-10 Expression Mediated by an Adeno-Associated Virus Vector Prevents Monocrotaline-Induced Pulmonary Arterial Hypertension in Rats

Takayuki Ito, Takashi Okada, Hiroshi Miyashita, Tatsuya Nomoto, Mutsuko
Nonaka-Sarukawa, Ryosuke Uchibori, Yoshikazu Maeda, Masashi Urabe, Hiroaki
Mizukami, Akihiro Kume, Masafumi Takahashi, Uichi Ikeda, Kazuyuki Shimada and
Keiya Ozawa

Circ. Res. 2007;101;734-741; originally published online Aug 2, 2007;

DOI: 10.1161/CIRCRESAHA.107.153023

Circulation Research is published by the American Heart Association, 7272 Greenville Avenue, Dallas,
TX 75214

Copyright © 2007 American Heart Association. All rights reserved. Print ISSN: 0009-7330. Online
ISSN: 1524-4571

The online version of this article, along with updated information and services, is
located on the World Wide Web at:
<http://circres.ahajournals.org/cgi/content/full/101/7/734>

Subscriptions: Information about subscribing to Circulation Research is online at
<http://circres.ahajournals.org/subscriptions/>

Permissions: Permissions & Rights Desk, Lippincott Williams & Wilkins, a division of Wolters
Kluwer Health, 351 West Camden Street, Baltimore, MD 21202-2436. Phone: 410-528-4050. Fax:
410-528-8550. E-mail:
journalpermissions@lww.com

Reprints: Information about reprints can be found online at
<http://www.lww.com/reprints>

Interleukin-10 Expression Mediated by an Adeno-Associated Virus Vector Prevents Monocrotaline-Induced Pulmonary Arterial Hypertension in Rats

Takayuki Ito, Takashi Okada, Hiroshi Miyashita, Tatsuya Nomoto, Mutsuko Nonaka-Sarukawa, Ryosuke Uchibori, Yoshikazu Maeda, Masashi Urabe, Hiroaki Mizukami, Akihiro Kume, Masafumi Takahashi, Uichi Ikeda, Kazuyuki Shimada, Keiyo Ozawa

Abstract—Pulmonary arterial hypertension (PAH) is a fatal disease associated with inflammation and pathological remodeling of the pulmonary artery (PA). Interleukin (IL)-10 is a pleiotropic antiinflammatory cytokine with vasculoprotective properties. Here, we report the preventive effects of IL-10 on monocrotaline-induced PAH. Three-week-old Wistar rats were intramuscularly injected with an adeno-associated virus serotype 1 vector expressing IL-10, followed by monocrotaline injection at 7 weeks old. IL-10 transduction significantly improved survival rates of the PAH rats 8 weeks after monocrotaline administration compared with control gene transduction (75% versus 0%, $P < 0.01$). IL-10 also significantly reduced mean PA pressure (22.8 ± 1.5 versus 29.7 ± 2.8 mm Hg, $P < 0.05$), a weight ratio of right ventricle to left ventricle plus septum (0.35 ± 0.04 versus 0.42 ± 0.05 , $P < 0.05$), and percent medial thickness of the PA ($12.9 \pm 0.3\%$ versus $21.4 \pm 0.4\%$, $P < 0.01$) compared with controls. IL-10 significantly reduced macrophage infiltration and vascular cell proliferation in the remodeled PA in vivo. It also significantly decreased the lung levels of transforming growth factor- β_1 and IL-6, which are indicative of PA remodeling. In addition, IL-10 increased the lung level of heme oxygenase-1, which strongly prevents PA remodeling. In vitro analysis revealed that IL-10 significantly inhibited excessive proliferation of cultured human PA smooth muscle cells treated with transforming growth factor- β_1 or the heme oxygenase inhibitor tin protoporphyrin IX. Thus, IL-10 prevented the development of monocrotaline-induced PAH, and these results provide new insights into the molecular mechanisms of human PAH. (*Circ Res.* 2007;101:734-741.)

Key Words: pulmonary hypertension ■ interleukins ■ gene therapy ■ inflammation
■ vascular smooth muscle cell proliferation

Pulmonary arterial hypertension (PAH) is an intractable disease that leads to increased pulmonary arterial pressure, progressive right heart failure, and premature death; however, no satisfactory treatment for PAH has been established.¹ The pathological process of PAH is characterized by abnormal remodeling of the pulmonary artery (PA) associated with excessive proliferation of pulmonary arterial smooth muscle cells (PASMCs).² Accumulating evidence suggests important roles of vascular inflammation in its pathogenesis.^{2,3} For instance, serum levels of proinflammatory cytokines such as interleukin (IL)-1 and IL-6 reflect the disease activity in patients with idiopathic PAH.⁴ Furthermore, injection of IL-6 can produce PAH and PA remodeling in rats.⁵ The remodeled PA presents macrophage infiltration and increased expression of a variety of cytokines, including IL-6, tumor necrosis factor (TNF)- α , and transforming

growth factor (TGF)- β_1 .^{6,7} Administration of steroids or immunosuppressive drugs decreases the level of PA pressure in patients with PAH.^{8,9} These observations suggest a therapeutic potential of targeting inflammation to prevent PAH progression.¹⁰ However, the precise mechanisms underlying the antiinflammatory effects on PA remodeling have not yet been fully investigated.

IL-10 is a multifunctional antiinflammatory cytokine with a vasculoprotective property. During the course of inflammation, IL-10 is produced by type-2 helper T (Th2) lymphocytes, and it inhibits the production of various proinflammatory cytokines in macrophages and Th1 lymphocytes.¹¹ Exogenous IL-10 prevents proliferative vasculopathy in vivo by inhibiting inflammatory cell infiltration,¹² smooth muscle cell proliferation,^{12,13} and chemokine expression.¹⁴ However, clinical efficacy of systemic recombinant IL-10 administra-

Original received March 28, 2007; revision received July 12, 2007; accepted July 23, 2007.

From the Division of Genetic Therapeutics (T.I., T.N., M.N.-S., M.U., H.M., A.K., K.O., R.U.), the Division of Cardiovascular Medicine (T.I., H.M., M.N.-S., K.S., Y.M.), Jichi Medical University, Japan; the Department of Molecular Therapy (T.O.), National Institute of Neuroscience, National Center of Neurology and Psychiatry, Japan; and the Department of Organ Regeneration (M.T., U.I.), Shinshu University Graduate School of Medicine, Japan.

Correspondence to Takayuki Ito, MD, PhD, Division of Genetic Therapeutics, Jichi Medical University, 3311-1 Yakushiji, Shimotsuke, Tochigi 329-0498, Japan. E-mail titou@jichi.ac.jp

© 2007 American Heart Association, Inc.

Circulation Research is available at <http://circres.ahajournals.org>

DOI: 10.1161/CIRCRESAHA.107.153023

Downloaded from circres.ahajournals.org at Shizuoka University Medical Library on April 10, 2008

tion are insufficient because of the lower local IL-10 levels resulting from its short bioactive half-life.¹⁵ In this study, we used an adeno-associated virus (AAV) vector for IL-10 expression because it is an efficient vehicle for systemic and sustained expression of therapeutic proteins.¹⁴ It also has an advantage over other viral vectors in the therapeutic or mechanistic analysis because it produces minimal inflammatory and immune responses *in vivo*.

Recently, heme oxygenase (HO)-1, an inducible form of HO that promotes production of a vasodilator carbon monoxide (CO), was shown to mediate antiinflammatory and antiproliferative effects of IL-10 in a model of chronic vasculopathy.¹² Increased HO-1 and CO levels attenuated PAH and PA remodeling by inhibiting PASMC proliferation.^{16–18} However, no study has explored a direct link between IL-10 and HO-1 in the pathogenesis of PAH. Thus, we examined the effects of IL-10, delivered via an AAV vector, on PA remodeling in a widely-used rat model of PAH induced by the pyrrolizidine alkaloid monocrotaline (MCT). We also investigated the mechanisms underlying the effects of IL-10 on the following factors involved in the inflammatory and proliferative vascular changes in PAH: PASMC, macrophage, TGF- β_1 , IL-6, and HO-1.

Materials and Methods

AAV Vector Production

DNA encoding rat IL-10 was polymerase chain reaction-amplified from rat splenocyte complementary DNA, using the primers 5'-GCACGAGAGCCACAACGCA-3' and 5'-GATTTGAGTACGATCCATTTATTCAAACGAGGAT-3'. For efficient transgene expression in the skeletal muscle, we constructed a recombinant AAV vector which carried the IL-10 gene (AAV-IL-10) or enhanced green fluorescent protein (eGFP) gene (AAV-eGFP), controlled by the modified chicken β -actin promoter with the cytomegalovirus-immediate early enhancer and the woodchuck hepatitis virus post-transcriptional regulatory element (a kind gift from Dr Thomas Hope, Infectious Disease Laboratory, Salk Institute). AAV vectors were prepared according to the previously described 3-plasmid transfection adenovirus-free protocol with minor modifications to use the active gassing system.^{19,20} In brief, 60% confluent human embryonic kidney 293 cells incubated in a large culture vessel with active air circulation were cotransfected with the proviral transgene plasmid, AAV-1 chimeric helper plasmid (p1RepCap), and adenoviral helper plasmid pAdeno (Avigen Inc). The crude viral lysate was purified by 2 rounds of cesium chloride 2-tier centrifugation.²¹ The viral stock titer was determined against plasmid standards by dot blot hybridization, after which the stock was dissolved in HN buffer (50 mmol/L HEPES, pH 7.4, 0.15 mol/L NaCl) before injection.

Animal Models

All animal experiments were approved by the Jichi Medical University ethics committee and were performed in accordance with the *National Institute of Health Guide for the Care and Use of Laboratory Animals*. To evaluate the efficiency of *in vivo* gene expression, 3-week-old male Wistar rats (Clea Japan Inc, Tokyo, Japan) weighing 45 to 55 g were injected with AAV-IL-10 (200 μ L, 3×10^{10} to 1×10^{11} genome copies [g.c.] per body) into the bilateral anterior tibial muscles (n=3 animals per group). For hemodynamic and histological analysis, we randomly formed 4 groups comprising 5 rats each: sham rats that were administered the HN buffer (1, NC group); MCT-treated rats administered the HN buffer (2, MCT group); MCT rats administered AAV-eGFP (3, MCT+eGFP group); and MCT rats administered AAV-IL-10 (4, MCT+IL-10 group). After anesthetized with a spontaneous inhalation of 1% isoflurane, the rats in the groups 3 and 4 received intramuscular injection of AAV-eGFP or

AAV-IL-10 (200 μ L, 6×10^{10} g.c. per body), respectively. Rats in groups 1 and 2 were injected with the HN buffer (200 μ L). MCT (Wako Pure Chemicals) was dissolved in 0.1N HCl, and the pH adjusted to 7.4 with 1.0N NaOH. For hemodynamic and histological studies, all rats except those in the NC group were subcutaneously injected with MCT (30 mg/kg) under the spontaneous inhalation of 1% isoflurane at 4 weeks after vector treatment. For the survival study, rats (n=8 animals/group) were injected with a lethal dose of MCT (45 mg/kg) under the spontaneous inhalation of 1% isoflurane at 4 weeks after vector injection. Survival was estimated from the date of MCT injection until death or 8 weeks after injection.

Hemodynamic Analysis

Four weeks after MCT injection, the rats were anesthetized with spontaneous inhalation of 1% isoflurane, and a tracheotomy was performed. Then, they were mechanically ventilated using a respirator (SAR-830/AP, CWE; tidal volume: 10 mL/kg, respiratory rate: 30 breaths per min) and anesthetized with 0.5% isoflurane through a tracheostomy. After the thoracic cavity was opened using a midsternal approach, 2.0F high-fidelity manometer-tipped catheters (SPC-320, Millar Instruments Inc) were inserted directly into the right or left ventricle. The mean pulmonary arterial pressure (mPAP) or mean aortic arterial pressure (mAoP) was measured using the catheters that were advanced from the right or left ventricle, respectively. The heart rate (HR) was measured by unipolar lead electrocardiography.

Ventricular Weight Measurement and Morphometric Analysis of the PA

After hemodynamic analysis, the rats were euthanized using an overdose isoflurane (5%). The lungs and PAs were perfused with 5 mL of saline followed by 10 mL of cold 4% paraformaldehyde. Each ventricle and the lungs were excised, dissected free, and weighed. The weight ratio of right ventricle to the left ventricle plus septum [RV/(LV+S)] was calculated as an index of right ventricular hypertrophy (RVH). The tissues were fixed in 4% paraformaldehyde for 4 hours, transferred to 30% sucrose in 0.1 mol/L phosphate buffer (pH 7.4) for cryoprotection, and stored at 4°C overnight. Lung tissue was frozen in Tissue-Tek OCT compound (Sakura Finetechnical Co) at -20°C. Then, 7- μ m sections were cut using a cryostat. Hematoxylin and eosin (HE) staining was performed on sections from the middle lobe of the right lung, and these were examined using light microscopy. Morphometric analysis was performed in PAs with an external diameter of 25 to 50 and 51 to 100 μ m. The medial wall thickness was calculated with the following formula: medial thickness (%) = medial wall thickness/external diameter \times 100.²² For quantitative analysis, 30 vessels from each rat were counted and the average was calculated.

Immunohistochemistry

Immunohistochemical staining was performed with monoclonal antibodies against ED1 (1:100; Serotec) and proliferating cell nuclear antigen (PCNA, 1:200; Zymed), using the streptavidin-biotin-peroxidase method, as described previously.²³ ED1 recognizes the lysosomal membrane antigen expressed by a majority of tissue macrophages. Irrelevant mouse immunoglobulin G (Vector Laboratories) was used as a negative control. Reactions were visualized using Vector SG (Vector Laboratories) or 3,3'-diaminobenzidine (Zymed) and counterstained with nuclear fast red or hematoxylin. The number of ED1-positive cells was counted in 250 \times 250- μ m fields under 400 \times magnification and expressed as cells per mm². The number of PCNA-positive cells was quantitatively evaluated as a percentage of total vascular cells in the fields under 1000 \times magnification. For each rat, the average number or percentage of each cell in 15 randomly selected fields was used for statistical analysis.

Protein Assay

Protein samples were prepared by homogenization of the frozen lung tissue in lysis buffer [10 μ mol/L Tris/Cl (pH 8.0), 0.2% NP-40,

1 $\mu\text{mol/L}$ EDTA (pH 7.6) supplemented with protease inhibitor cocktail Complete Mini (Roche Diagnostics). After centrifugation of the homogenates (3000g for 10 minutes), the supernatants or serum samples were used for measurement. To activate latent TGF- β_1 to an immunoreactive form, the samples were treated with acid according to the manufacturer's instructions (R&D Systems Inc). IL-10 or IL-6 concentrations in the sera and TGF- β_1 , IL-6, HO-1, or TNF- α in the lung extracts were measured using enzyme-linked immunosorbent assay (ELISA) kits (Amersham Pharmacia Biotech; R&D Systems). The minimum detectable dose was 3, 3, 16, and 5 pg/mL or 0.78 ng/mL for IL-10, TGF- β_1 , IL-6, and TNF- α , or HO-1, respectively. Inter- and intraassay precision of these kits was <10%. The total protein concentrations in the lung extracts were estimated using a BCA Protein Assay kit (PIERCE). The levels of TGF- β_1 , IL-6, HO-1, or TNF- α in the lung were expressed as pg per mg protein.

Cell Culture and Proliferation Assay

Human PSMCs were obtained from Clonetics Corp and grown in SmGM-2 medium (Clonetics Corp). PSMCs with a passage between 4 and 6 were used in the experiments. Cells (1×10^5 per well) were incubated in 96-well plates with serum-free Dulbecco's modified Eagle's medium and nutrient mixture F12 (DMEM-F12, Invitrogen) in an atmosphere of 5% CO₂ in the air at 37°C. A tetrazolium-based colorimetric proliferation assay (XTT assay; Cell Proliferation Kit II, Roche Diagnostics) was performed 2 days after adding tin protoporphyrin IX (SnPP; Frontier Scientific), human recombinant TGF- β_1 , IL-6, or IL-10 (PeproTech Inc). The optical density between 450 and 650 nm were measured to estimate the number of viable cells.

Statistical Analysis

Data from multiple experiments are expressed as mean \pm SEM. Statistical analysis and correlations were performed using StatView (Abacus Concepts, Inc). Survival curves were analyzed using the Kaplan-Meier method and compared by log-rank tests. Differences in other parameters were evaluated by analysis of variance combined with Fisher test. The correlation test was used to measure the association between 2 variables. A value of $P < 0.05$ was considered statistically significant.

Results

AAV Vector-Mediated IL-10 Expression Improves Survival of MCT-PAH Rats

Eight weeks after AAV-IL-10 injection, serum IL-10 concentrations were elevated in a vector dose-dependent manner (Figure 1A). We determined that injection with AAV-IL-10 (6×10^{10} g.c. per rat) significantly increased serum IL-10 levels as compared with untreated controls (184.1 ± 47.6 versus 18.8 ± 1.3 pg/mL, $P < 0.05$, $n = 3$ each). In contrast, injection with MCT (Figure 1A) or AAV-eGFP alone (data not shown) caused no significant change in serum IL-10 levels. Therefore, we used this dosage for all vectors in subsequent experiments. For survival analysis, the rats were injected with a lethal dose of MCT, after 4 weeks of vector injection. The survival in IL-10-transduced rats was significantly improved as compared with the eGFP-transduced rats 8 weeks after MCT injection (75% versus 0%, $P < 0.01$, $n = 8$ each; Figure 1B).

Effects of IL-10 on PAH and RVH

Four weeks after MCT injection, the mPAP levels were significantly higher than those of the untreated controls (30.1 ± 4.0 versus 20.0 ± 2.1 mm Hg, $P < 0.01$, $n = 5$ each; Figure 2A). Treatment with AAV-IL-10 but not AAV-eGFP significantly inhibited the elevation of mPAP (22.8 ± 1.5

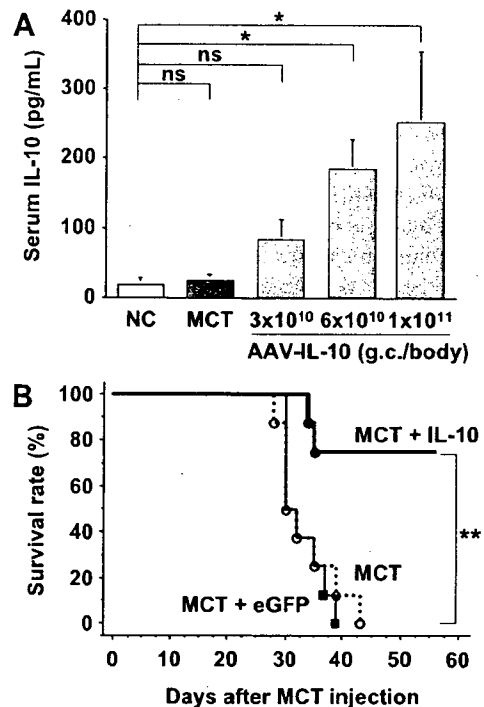


Figure 1. Adeno-associated virus (AAV) vector-mediated systemic interleukin (IL)-10 expression improves survival of monocrotaline (MCT)-induced pulmonary arterial hypertension (PAH) rats. **A**, In vivo IL-10 expression induced by AAV-IL-10. Serum IL-10 concentrations (pg/mL) were determined using ELISA 8 weeks after a single intramuscular injection of AAV-IL-10 into the anterior tibial muscles of 3-week-old Wistar rats. Genome copies (g.c.) per rat were as indicated. Data represent mean \pm SEM ($n = 3$ animals per group, $*P < 0.05$). ns indicates not statistically significant; NC, untreated controls. **B**, The Kaplan-Meier survival curve in MCT-PAH rats. The Wistar rats were treated with a lethal dose of MCT 4 weeks after the single intramuscular injection of HN buffer (MCT group), AAV-eGFP (MCT + eGFP group), or AAV-IL-10 (MCT + IL-10 group). $n = 8$ animals per group, $**P < 0.01$ versus MCT or MCT + eGFP groups.

versus 29.7 ± 2.8 mm Hg, $P < 0.01$, $n = 5$ each; Figure 2A). Moreover, serum IL-10 concentrations correlated negatively with mPAP in MCT-treated rats ($r = -0.75$, $P < 0.01$, $n = 15$; Figure 2B). In contrast, this IL-10 expression caused no significant change in HR (data not shown) and mAoP (76.7 ± 2.1 versus 74.6 ± 6.8 mm Hg, MCT + IL-10 versus MCT + eGFP group, $n = 5$ each). IL-10 expression also has a beneficial effect on RVH. Four-week MCT treatment significantly increased the RV/(LV+S) values as compared with the untreated controls ($P < 0.01$, $n = 5$ each; Figure 2C). Treatment with AAV-IL-10 but not AAV-eGFP inhibited MCT-induced increase of RV/(LV+S) significantly ($P < 0.05$, $n = 5$ each; Figure 2C). Furthermore, serum IL-10 concentrations correlated negatively with RV/(LV+S) in MCT-treated rats ($r = -0.57$, $P < 0.05$, $n = 15$; Figure 2D). These results indicate that sustained IL-10 expression prevented the development of MCT-induced PAH and RVH.

Effects of IL-10 on Histological Changes of the PA

Medial hypertrophy is a hallmark of pathological vascular remodeling in PAH. Four weeks after MCT injection, the medial thickness of PAs was markedly increased in the MCT-treated rats compared with untreated controls ($P < 0.01$,

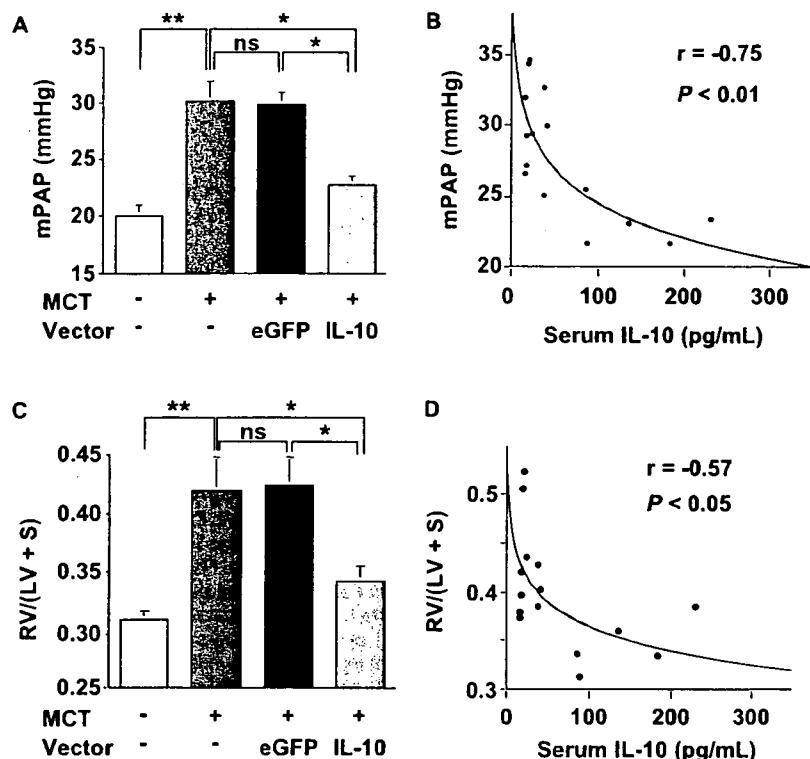


Figure 2. Effects of IL-10 on PAH and right ventricular hypertrophy (RVH). The 7-week-old Wistar rats were treated with monocrotaline (MCT) 4 weeks after vector injection. **A**, Statistical analysis of mean pulmonary arterial pressure (mPAP, mmHg) determined by direct catheterization 4 weeks after MCT injection. Data represent the mean \pm SEM ($n=5$ animals per group; * $P<0.05$, ** $P<0.01$). ns indicates not statistically significant. **B**, Correlation between serum IL-10 concentrations and mPAP levels in the MCT-treated rats (groups: MCT, MCT+eGFP, or MCT+IL-10; $n=5$ animals per group; $r=-0.75$, $P<0.01$). **C**, Quantitative RVH analysis. The weight ratio of the right ventricle to left ventricle plus septum [RV/(LV+S)] is presented as an index of RVH ($n=5$ animals per group; * $P<0.05$, ** $P<0.01$). **D**, Correlation between serum IL-10 concentrations and RV/(LV+S) in the MCT-treated rats (groups: MCT, MCT+eGFP, and MCT+IL-10; $n=5$ animals per group; $r=-0.57$, $P<0.05$).

$n=5$ each; Figure 3B, 25 to 50 μm ; Figure 3C, 51 to 100 μm in external diameter). Treatment with AAV-IL-10 but not AAV-eGFP significantly inhibited the increase in percent medial thickness ($P<0.01$, $n=5$ each). Inflammatory cell infiltration and vascular cell proliferation are also important indicators in the progression of PA remodeling. Immunohistochemical analysis shows that treatment with AAV-IL-10 significantly decreased the number of accumulated macrophages (ED1-positive cells; $P<0.01$, $n=5$ each; Figure 3D) and proliferating vascular cells (PCNA-positive cells; $P<0.01$, $n=5$ each; Figure 3E) in the PA of MCT-treated rats as compared with treatment with MCT alone or AAV-eGFP.

Effects of IL-10 on Cytokine Expression

We analyzed pulmonary tissue and serum cytokine levels relevant to the pathogenesis of PAH. Four weeks after MCT injection, the TGF- β_1 and IL-6 levels in the MCT-treated rats were significantly higher than those of the untreated controls ($P<0.01$, $n=5$ each; Figure 4A and 4C). Treatment with AAV-IL-10 but not AAV-eGFP significantly inhibited the MCT-induced elevation of TGF- β_1 and IL-6 levels ($P<0.01$, $n=5$ each). Furthermore, these levels correlated positively with the percent medial thickness in the rats with or without MCT treatment ($r=0.84$, $P<0.01$; $r=0.87$, $P<0.01$, respectively; Figure 4B and 4D).

HO-1 has been reported to mediate the antiinflammatory effects of IL-10.²⁴ Treatment with AAV-IL-10 but not AAV-eGFP or MCT alone significantly increased the lung HO-1 levels as compared with untreated controls ($P<0.05$, $n=5$ each, Figure 4E). In addition, HO-1 levels correlated negatively with IL-6 levels in MCT-treated rats ($r=-0.85$, $P<0.01$; Figure 4F). In contrast, serum IL-6 levels positively correlated with lung IL-6 levels ($r=-0.69$, $P<0.01$; Figure

4G). Although the lung TNF- α levels significantly increased in MCT-treated rats compared with untreated controls, IL-10 expression caused no change in the lung TNF- α levels (Figure 4H).

Effects of IL-10 on PASMC Proliferation

To determine whether IL-10 directly inhibits PASMC proliferation, we performed an in vitro colorimetric XTT assay using cultured human PASMCs. Treatment of PASMCs with SnPP, which inactivates HO-1, and treatment with TGF- β_1 or IL-6 dose dependently promoted cell proliferation ($n=4$ each, $P<0.05$; Figure 5A through 5C). Treatment with IL-10 alone had no significant effect on PASMC proliferation (Figure 5D). On the other hand, pretreatment with IL-10 significantly inhibited PASMC proliferation induced by SnPP or TGF- β_1 ($n=4$ each, $P<0.05$; Figure 5E) but not that induced by IL-6.

Discussion

The present study demonstrates that IL-10, delivered by an intramuscular injection of an AAV1 vector, prevented the development of MCT-PAH in rats. Systemic IL-10 expression also improved survival in rats and prevented the development of RVH and medial hypertrophy of PA. IL-10 also reduced macrophage accumulation, vascular cell proliferation, and pulmonary tissue levels of TGF- β_1 and IL-6, all of which play pivotal roles in progression of PA remodeling. Further, IL-10 enhanced HO-1 levels in the lung. Thus, IL-10 exerts multiple preventive effects on inflammatory and proliferative PA remodeling (Figure 6).

Blockade of a single proinflammatory signaling pathway by IL-1 or monocyte chemoattractant protein-1 attenuates PA remodeling.^{25,26} However, the prosurvival effects of antiinflammatory molecules on PAH animals have not been re-

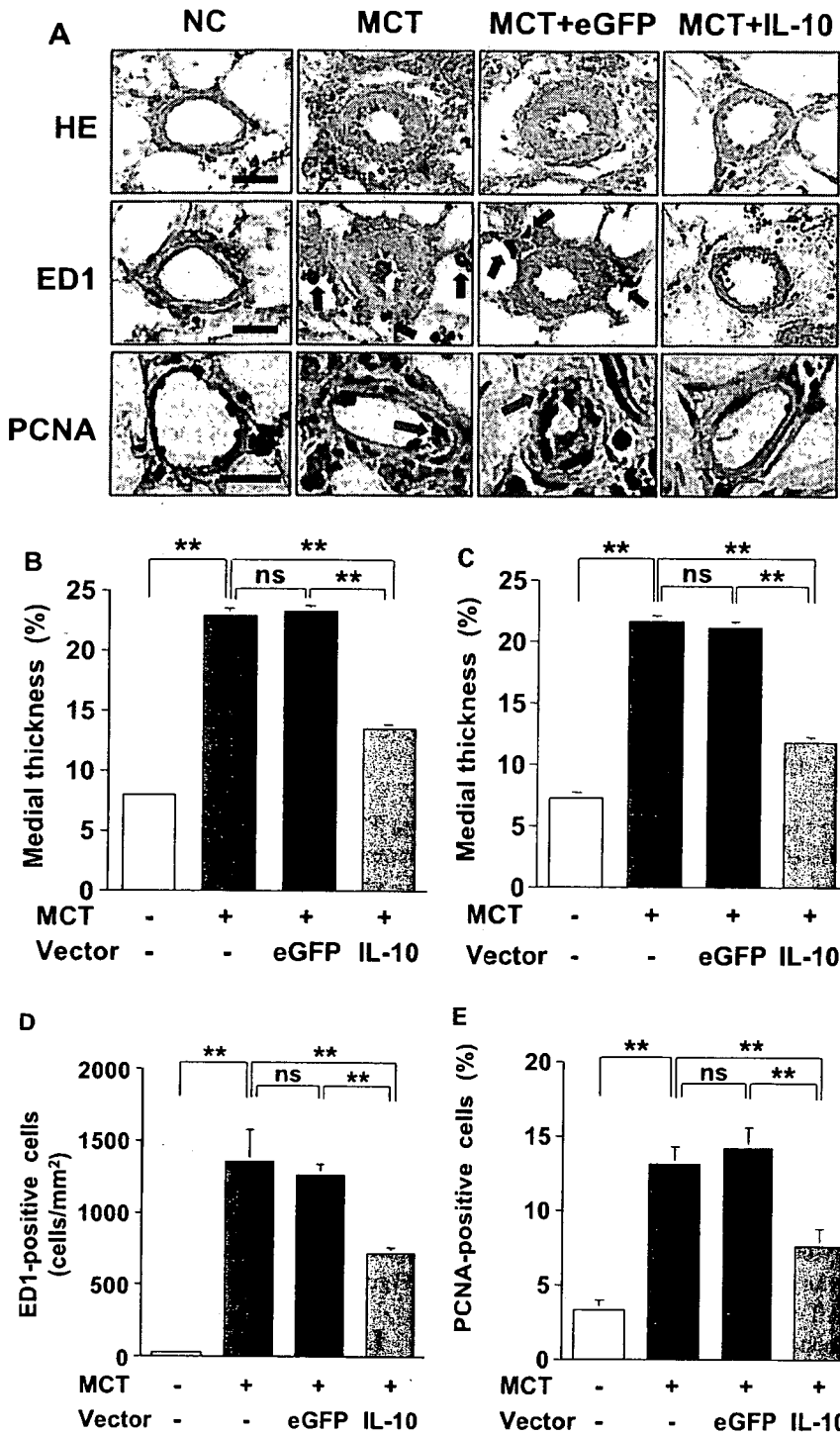


Figure 3. Antiinflammatory and antiproliferative effects of IL-10 on the remodeled pulmonary artery (PA). The 7-week-old Wistar rats were treated with MCT 4 weeks after vector injection. Representative cross-sectional views of the peripheral PAs stained with HE or immunohistochemistry (ED1 or PCNA) 4 weeks after MCT treatment (A; original magnification $\times 1000$, Scale bar = $20 \mu\text{m}$). Blue arrows indicate ED-1-positive cells and red arrows, PCNA-positive cells. Quantification of percent medial thickness for vessels 25 to 50 μm (B) and 51 to 100 μm (C) in external diameter. Quantitative analysis of the number of perivascular macrophages (ED-1-positive cells, D) and proliferating vascular cells (PCNA-positive cells, E). Data represent mean \pm SEM (n = 5 animals per group, $**P < 0.01$). ns indicates not statistically significant.

ported. Evidence of right heart failure is involved in the mortality of MCT-PAH rats. In this study, all rats treated with a lethal dose of MCT exhibited symptoms of right heart failure such as pleural effusion and body weight decrease. In the setting of severe PAH and right heart failure, cytokine networks may orchestrate disease progression. Thus, blockades of multiple inflammatory signals might be responsible for the prosurvival effect of IL-10.

IL-10 has gained significant attention because of its suppressive influence on inflammatory and proliferative vasculopathy. The IL-10 receptor is expressed on vascular smooth

muscle cells (VSMCs). IL-10 inhibits inflammation and VSMC proliferation in arterial remodeling after balloon injury or transplant rejection.^{12,13} Consistent with previous studies using MCT-PAH,^{6,7} we demonstrate that increased levels of TGF- β_1 and IL-6 are related to PASMCM proliferation and PA remodeling progression. Although treatment with IL-10 alone caused no significant effects on PASMCM proliferation,²⁷ IL-10 significantly inhibited the lung TGF- β_1 expression and TGF- β_1 -induced PASMCM proliferation. TGF- β_1 enhances PASMCM proliferation of idiopathic PAH patients but not that of normal subjects or secondary PAH patients.²⁸

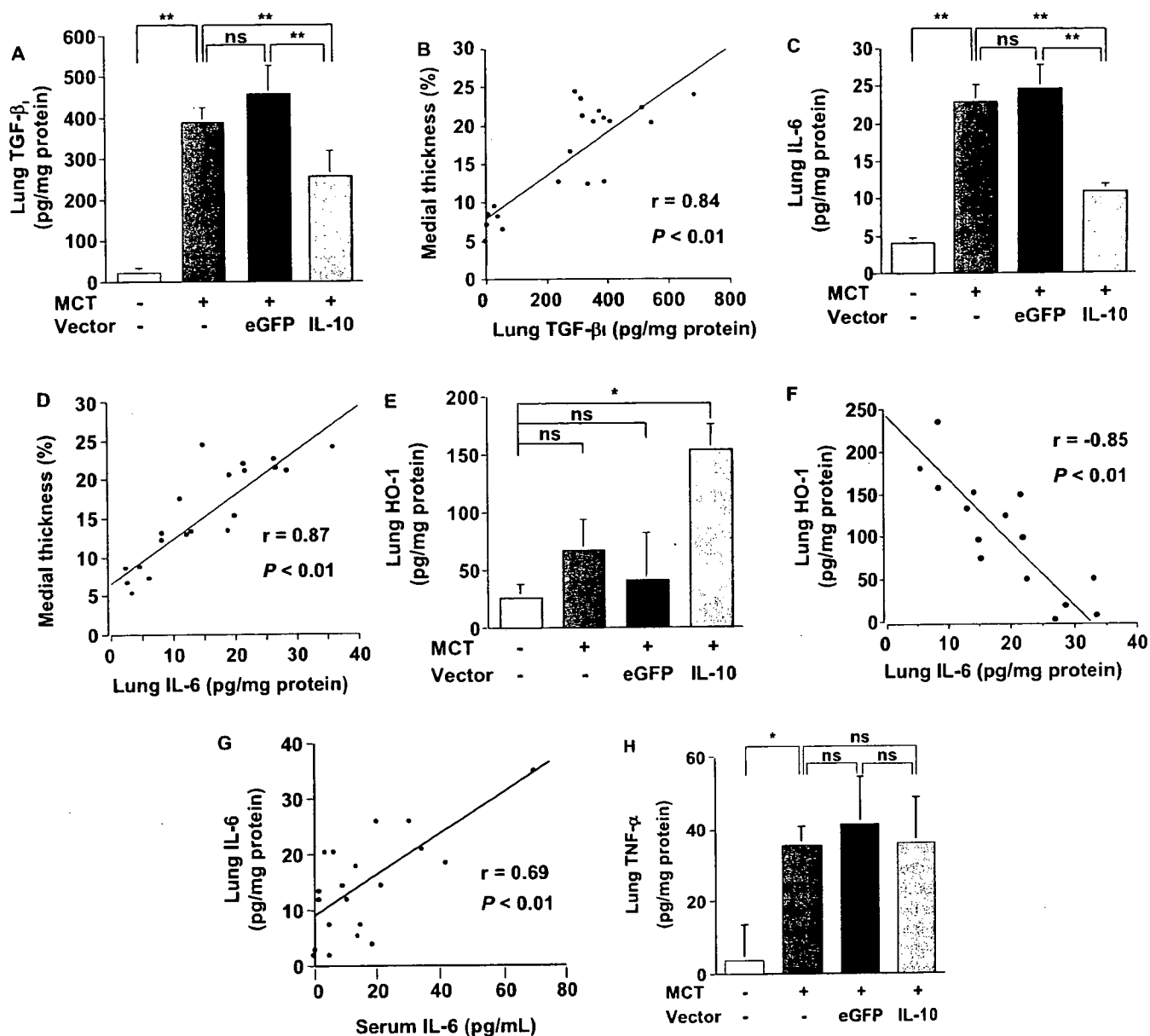


Figure 4. Effects of IL-10 on expression of transforming growth factor-β₁ (TGF-β₁), IL-6, heme oxygenase-1 (HO-1), and tumor necrosis factor-α (TNF-α) in the lung. The 7-week-old Wistar rats were treated with MCT 4 weeks after vector injection. Concentrations of active TGF-β₁ (A), IL-6 (C), HO-1 (E), and TNF-α (H) in the lung extracts were detected using ELISA 4 weeks after MCT treatment. Data represent mean ± SEM (n=5 animals per group; *P<0.05, **P<0.01). ns indicates not statistically significant. Correlation between the percent medial thickness and lung levels of TGF-β₁ (B) or IL-6 (D) in rats (groups: NC, MCT, MCT+eGFP, or MCT+IL-10; n=5 animals per group; r=0.84, P<0.01 and r=0.87, P<0.01, respectively). Correlation between the HO-1 and IL-6 (F) levels in the rat lung (groups: MCT, MCT+eGFP, or MCT+IL-10; n=5 animals per group; r=-0.85, P<0.01). Correlation between the lung and serum IL-6 levels (G) in rats (groups: NC, MCT, MCT+eGFP, or MCT+IL-10; n=5 animals per group; r=0.69, P<0.01).

Additionally, TGF-β₁ is accumulated in the hypertrophic PA of both human PAH and MCT-PAH^{29,30} and exacerbates PA remodeling.³¹

IL-6, a multifunctional proinflammatory cytokine, acts as a strong mitogen to promote VSMC proliferation.¹¹ Macrophage infiltration is a hallmark of PAH progression, and activated macrophages produce substantial amounts of IL-6 in MCT-PAH rats.^{6,32} In this study, IL-10 treatment inhibited perivascular macrophage infiltration and the lung IL-6 expression in vivo but not IL-6-induced PASM proliferation in vitro. These results suggest that IL-10 may attenuate IL-6 function indirectly through the decreased accumulation of perivascular macro-

phages and IL-6. Furthermore, the serum IL-6 levels significantly correlated with the lung IL-6 levels. Because serum IL-6 level reflects the disease activity of idiopathic PAH, it can be a useful biomarker of antiinflammation therapy of PAH. On the other hand, IL-10 did not affect the MCT-induced TNF-α expression in the lung. However, previous studies demonstrated that IL-10 prevents TNF-α-induced VSMC proliferation in vitro.²⁷ These observations suggest that IL-10 might modulate the downstream signal of TNF-α but not its expression in the setting of MCT-PAH. Overall, IL-10 affects the dynamics of cytokine networks involved in PA remodeling, and its site of action may differ according to the cytokine signal.

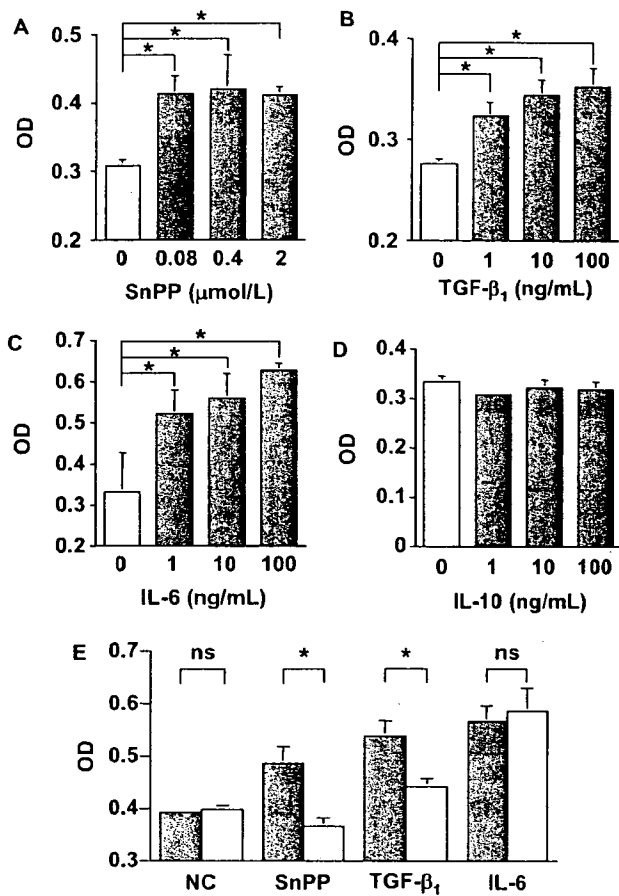


Figure 5. Antiproliferative effects of IL-10 on pulmonary arterial smooth muscle cells (PASMCs). The number of viable human PASMCs cultured in serum-free DMEM-F12 was estimated using a colorimetric assay (XTT assay). The optical density (OD) between 450 nm and 650 nm indicates the extent of cell proliferation. Addition of tin protoporphyrin IX (SnPP, A), TGF- β_1 (B), or IL-6 (C) dose-dependently promotes PASMC proliferation. Although IL-10 alone has no significant effect (D), pretreatment with IL-10 (10 ng/mL) inhibits PASMC proliferation induced by SnPP (2 μ mol/L) or TGF- β_1 (20 ng/mL, E) but not that induced by IL-6 (20 ng/mL). Closed columns, cells not treated with IL-10; open columns, IL-10-treated cells. The results are representative of 3 independent experiments. Data represent mean \pm SEM (n=4 each, *P<0.05). ns indicates not statistically significant.

CO induced by HO-1 blocks PASMC proliferation not only directly by inhibiting the expression of a cell cycle-specific transcription factor but also indirectly by attenuating mitogen signaling.¹⁶ Interestingly, the transgenic mice that constitutively express HO-1 are protected from the development of hypoxia-induced PAH and excessive expression of a mitogen IL-6.³³ In this study, AAV-IL-10 administration increased the HO-1 level that negatively correlated with the IL-6 level in the lung of MCT-PAH rats. These observations suggest a dynamic relationship between IL-6 and HO-1 in PA remodeling progression. Chen et al¹² reported that AAV-IL-10 injection enhanced the activity and protein levels of HO-1, but SnPP treatment that inactivates HO-1 reversed the vasculoprotective effects of IL-10 in vivo. Here, we show that pretreatment with recombinant IL-10 suppressed the excessive PASMC proliferation induced by HO-1 inactivation with SnPP. Thus, IL-10 may sustain CO levels by maintaining

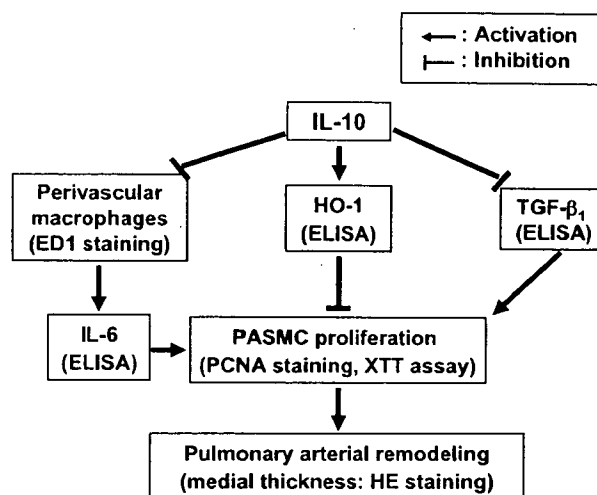


Figure 6. Proposed explanation for IL-10-mediated prevention of PAH and vascular remodeling. Monocrotaline treatment causes PAH in rats by inducing inflammation and proliferation of the PA. IL-10 prevents the development of PAH and PA remodeling by inhibiting vascular inflammation and proliferation. The effects of IL-10 are related to the decreased accumulation of perivascular macrophages and the reduced levels of active TGF- β_1 and IL-6. IL-10 induces HO-1 expression, which can negatively regulate inflammation and proliferation in the PA. IL-10 inhibits abnormal proliferation of PSMCs, thereby preventing PAH development.

HO-1 from inactivating, leading to the prevention of PA remodeling.

Finally, we will discuss the clinical implication and limitations of this study. Consistent with previous studies, maximum gene expression was noted 6 to 8 weeks after the intramuscular injection of AAV vectors. In this study, AAV-IL-10 was injected 4 weeks before MCT administration for the transgene expression to reach plateau levels when MCT-PAH was fully developed (3 to 4 weeks after the injection). Thus, our results are completely based on a prevention protocol, which may be rare in a clinical setting. Intramuscular AAV-IL-10 injection is an attractive candidate for antiinflammation therapy of PAH because inflammatory cytokine expression is associated with the clinical course of the disease. In addition, this strategy exhibited no life-threatening complications such as shock and sepsis which may occur in intravenous prostacyclin infusion therapy. However, therapeutic effects of IL-10 in established PAH has not been determined. Therefore, it should be further examined in studies using a treatment protocol. MCT-PAH is a widely-used and suitable model for exploring inflammatory mechanisms in PAH progression. However, how IL-10 affects other pathogenesis in PAH remains unknown. In the future, IL-10 function needs to be examined in other PAH models such as hypoxia-induced PAH.

In conclusion, AAV vector-mediated sustained IL-10 expression prevented the development of MCT-PAH in rats. The antiremodeling effects of IL-10 are related to the reduction of macrophage infiltration and pathological cytokine expression as well as increased HO-1 levels in the lung. Although the therapeutic role of IL-10 should be further investigated, our results provide new insights into molecular mechanisms underlying the development of human PAH.

Acknowledgments

We thank Miyoko Mitsu for her encouragement and technical support.

Sources of Funding

This work was supported by grants from (1) the Ministry of Health, Labor and Welfare of Japan; (2) Grants-in-Aid for Scientific Research; (3) grant for 21 Century COE Program; (4) "High-Tech Research Center" Project for Private Universities, matching fund subsidy, from the Ministry of Education, Culture, Sports, Science and Technology of Japan; and (5) The Research Award to Jichi Medical School Graduate Student.

Disclosures

None.

References

- Humbert M, Sitbon O, Simonneau G. Treatment of pulmonary arterial hypertension. *N Engl J Med*. 2004;351:1425–1436.
- Stenmark KR, Fagan KA, Frid MG. Hypoxia-induced pulmonary vascular remodeling: cellular and molecular mechanisms. *Circ Res*. 2006;99:675–691.
- Tuder RM, Groves B, Badesch DB, Voelkel NF. Exuberant endothelial cell growth and elements of inflammation are present in plexiform lesions of pulmonary hypertension. *Am J Pathol*. 1994;144:275–285.
- Humbert M, Monti G, Brenot F, Sitbon O, Portier A, Grangeot-Keros L, Duroux P, Galanaud P, Simonneau G, Emilie D. Increased interleukin-1 and interleukin-6 serum concentrations in severe primary pulmonary hypertension. *Am J Respir Crit Care Med*. 1995;151:1628–1631.
- Miyata M, Sakuma F, Yoshimura A, Ishikawa H, Nishimaki T, Kasukawa R. Pulmonary hypertension in rats. 2. Role of interleukin-6. *Int Arch Allergy Immunol*. 1995;108:287–291.
- Miyata M, Sakuma F, Yoshimura A, Ishikawa H, Nishimaki T, Kasukawa R. Pulmonary hypertension in rats. 1. Role of bromodeoxyuridine-positive mononuclear cells and alveolar macrophages. *Int Arch Allergy Immunol*. 1995;108:281–286.
- Arcot SS, Lipke DW, Gillespie MN, Olson JW. Alterations of growth factor transcripts in rat lungs during development of monocrotaline-induced pulmonary hypertension. *Biochem Pharmacol*. 1993;46:1086–1091.
- Karmochkine M, Wechsler B, Godeau P, Brenot F, Jagot JL, Simonneau G. Improvement of severe pulmonary hypertension in a patient with SLE. *Ann Rheum Dis*. 1996;55:561–562.
- Bellotto F, Chiavacci P, Lavceder F, Angelini A, Thiene G, Marcolongo R. Effective immunosuppressive therapy in a patient with primary pulmonary hypertension. *Thorax*. 1999;54:372–374.
- Ito T, Ozawa K, Shimada K. Current drug targets and future therapy of pulmonary arterial hypertension. *Curr Med Chem*. 2007;14:719–733.
- Ito T, Ikeda U. Inflammatory cytokines and cardiovascular disease. *Curr Drug Targets Inflamm Allergy*. 2003;2:257–265.
- Chen S, Kapturczak MH, Wasserfall C, Glushakova OY, Campbell-Thompson M, Deshane JS, Joseph R, Cruz PF, Hauswirth WW, Madsen KM, Croker BP, Berns KI, Atkinson MA, Flotte TR, Tisher CC, Agarwal A. Interleukin 10 attenuates neointimal proliferation and inflammation in aortic allografts by a heme oxygenase-dependent pathway. *Proc Natl Acad Sci U S A*. 2005;102:7251–7256.
- Mazighi M, Pelle A, Gonzalez W, Mtairag el M, Philippe M, Henin D, Michel JB, Feldman LJ. IL-10 inhibits vascular smooth muscle cell activation *in vitro* and *in vivo*. *Am J Physiol Heart Circ Physiol*. 2004;287:H866–H871.
- Yoshioka T, Okada T, Maeda Y, Ikeda U, Shimpō M, Nomoto T, Takeuchi K, Nonaka-Sarukawa M, Ito T, Takahashi M, Matsushita T, Mizukami H, Hanazono Y, Kume A, Ookawara S, Kawano M, Ishibashi S, Shimada K, Ozawa K. Adeno-associated virus vector-mediated interleukin-10 gene transfer inhibits atherosclerosis in apolipoprotein E-deficient mice. *Gene Ther*. 2004;11:1772–1779.
- Li MC, He SH. IL-10 and its related cytokines for treatment of inflammatory bowel disease. *World J Gastroenterol*. 2004;10:620–625.
- Morita T, Mitsialis SA, Koike H, Liu Y, Kourembanas S. Carbon monoxide controls the proliferation of hypoxic vascular smooth muscle cells. *J Biol Chem*. 1997;272:32804–32809.
- Christou H, Morita T, Hsieh CM, Koike H, Arkonac B, Perrella MA, Kourembanas S. Prevention of hypoxia-induced pulmonary hypertension by enhancement of endogenous heme oxygenase-1 in the rat. *Circ Res*. 2000;86:1224–1229.
- Yun S, Junbao D, Limin G, Chaomei Z, Xiuying T, Chaoshu T. The regulating effect of heme oxygenase/carbon monoxide on hypoxic pulmonary vascular structural remodeling. *Biochem Biophys Res Commun*. 2003;306:523–529.
- Matsushita T, Elliger S, Elliger C, Podoskoff G, Villarreal L, Kurtzman GJ, Iwaki Y, Colosi P. Adeno-associated virus vectors can be efficiently produced without helper virus. *Gene Ther*. 1998;5:938–945.
- Okada T, Nomoto T, Yoshioka T, Nonaka-Sarukawa M, Ito T, Ogura T, Iwata-Okada M, Uchibori R, Shimazaki K, Mizukami H, Kume A, Ozawa K. Large-scale production of recombinant viruses by use of a large culture vessel with active gassing. *Hum Gene Ther*. 2005;16:1212–1218.
- Okada T, Nomoto T, Shimazaki K, Lijun W, Lu Y, Matsushita T, Mizukami H, Urabe M, Hanazono Y, Kume A, Muramatsu S, Nakano I, Ozawa K. Adeno-associated virus vectors for gene transfer to the brain. *Methods*. 2002;28:237–247.
- Kay JM, Keane PM, Suyama KL, Gauthier D. Angiotensin converting enzyme activity and evolution of pulmonary vascular disease in rats with monocrotaline pulmonary hypertension. *Thorax*. 1982;37:88–96.
- Yoshioka T, Ageyama N, Shibata H, Yasu T, Misawa Y, Takeuchi K, Matsui K, Yamamoto K, Terao K, Shimada K, Ikeda U, Ozawa K, Hanazono Y. Repair of infarcted myocardium mediated by transplanted bone marrow-derived CD34⁺ stem cells in a nonhuman primate model. *Stem Cells*. 2005;23:355–364.
- Lee TS, Chau LY. Heme oxygenase-1 mediates the anti-inflammatory effect of interleukin-10 in mice. *Nat Med*. 2002;8:240–246.
- Voelkel NF, Tuder RM, Bridges J, Arend WP. Interleukin-1 receptor antagonist treatment reduces pulmonary hypertension generated in rats by monocrotaline. *Am J Respir Cell Mol Biol*. 1994;11:664–675.
- Kimura H, Kasahara Y, Kurosu K, Sugito K, Takiguchi Y, Terai M, Mikata A, Natsume M, Mukaida N, Matsushima K, Kuriyama T. Alleviation of monocrotaline-induced pulmonary hypertension by antibodies to monocyte chemoattractant and activating factor/monocyte chemoattractant protein-1. *Lab Invest*. 1998;78:571–581.
- Selzman CH, McIntyre RC Jr, Shames BD, Whitchill TA, Banerjee A, Harken AH. Interleukin-10 inhibits human vascular smooth muscle proliferation. *J Mol Cell Cardiol*. 1998;30:889–896.
- Morrell NW, Yang X, Upton PD, Jourdan KB, Morgan N, Sheares KK, Trembath RC. Altered growth responses of pulmonary artery smooth muscle cells from patients with primary pulmonary hypertension to transforming growth factor- β_1 and bone morphogenetic proteins. *Circulation*. 2001;104:790–795.
- Botney MD, Bahadori L, Gold LI. Vascular remodeling in primary pulmonary hypertension. Potential role for transforming growth factor- β . *Am J Pathol*. 1994;144:286–295.
- Tanaka Y, Schuster DP, Davis EC, Patterson GA, Botney MD. The role of vascular injury and hemodynamics in rat pulmonary artery remodeling. *J Clin Invest*. 1996;98:434–442.
- El-Haroun H, Bradbury D, Clayton A, Knox AJ. Interleukin-1 β , transforming growth factor- β_1 , and bradykinin attenuate cyclic AMP production by human pulmonary artery smooth muscle cells in response to prostacyclin analogues and prostaglandin E2 by cyclooxygenase-2 induction and downregulation of adenylyl cyclase isoforms 1, 2, and 4. *Circ Res*. 2004;94:353–361.
- Suzuki C, Takahashi M, Morimoto H, Izawa A, Ise H, Hongo M, Hoshikawa Y, Ito T, Miyashita H, Kobayashi E, Shimada K, Ikeda U. Mycophenolate mofetil attenuates pulmonary arterial hypertension in rats. *Biochem Biophys Res Commun*. 2006;349:781–788.
- Minamino T, Christou H, Hsieh CM, Liu Y, Dhawan V, Abraham NG, Perrella MA, Mitsialis SA, Kourembanas S. Targeted expression of heme oxygenase-1 prevents the pulmonary inflammatory and vascular responses to hypoxia. *Proc Natl Acad Sci U S A*. 2001;98:8798–8803.